OPT-MPC

Copernicus Sentinel

Optical Mission Performance Cluster

Customer:	ESA	**Document Ref.:**	OMPC.ACR.HBK.002
Contract No.:	4000111836/14/I-LG	**Date:**	14/04/2023
		Issue:	1.3

Project:	PREPARATION AND OPERATIONS OF THE MISSION PERFORMANCE CENTRE (MPC) FOR THE COPERNICUS SENTINEL-3 MISSION
Title:	Copernicus Sentinel-3 SLSTR Land User Handbook
Author(s):	E. Polehampton, C. Cox, D. Smith (RAL Space), D. Ghent (ULEIC), M. Wooster, W. Xu (KCL), J. Bruniquel), C. Henocq (ACRI-ST), S. Dransfeld (ESA)
Filename	Sentinel3-SLSTR-Land-Handbook - i1r3 - 14April2023.docx

Disclaimer

The work performed in the frame of this contract is carried out with funding by the European Union. The views expressed herein can in no way be taken to reflect the official opinion of either the European Union or the European Space Agency.

Changes Log

Version	Date	Changes
1.0	15/02/2021	First version
1.1	14/06/2021	Updated version to account for the new LST uncertainties and the evolution of the snow masking
1.2	14/09/2022	Updated version to account for removal of Probabilistic cloud flag in Level 1, and additional FAQs added.
1.3	14/04/2023	Updated version to account for FRP V2

List of Changes

Version	Section	Changes
1.1	5.1.1; 6.2.1	Snow masking evolution in LST processing
	5.1.1; 6.2.1	LST uncertainties evolution
1.2		Change of reference as the document is now maintained in the frame of the OPT-MPC contract. New reference is OMPC.ACR.HBK.002. For sake of traceability, issue en released Ids are kept.
	5.1.1; 7.3	LST uncertainty example and quality of the uncertainties
	6.1	Updated information to take into accunt filenaming changes (processor centre)
	8.2.1.6	FAQ item added on how to interpret pointing flags
	8.2.1.7	FAQ item added on how to find quality information in the product manifest
	8.2.1.8	FAQ item added on how to calculate per pixel uncertainty at Level 1
1.3	5.1.2	Addition of few information about SWIR fire detection
	6.2.1	Correction of a obsolete sentence regarding probabilistic cloud mask computed during SLSTR L1 module
	6.2.2	Update of the FRP section to be aligned with FRP V2 algorithm and products

Table of content

1 Introduction

This Copernicus Sentinel-3 SLSTR Land User Handbook aims to provide a summary of key information needed for users interested in SLSTR land products and their applications.

After providing a general introduction to the Copernicus programme, the role of the European Space Agency and the scope of the Sentinel-3 mission, it gives detailed information about SLSTR products: the algorithms, processing levels, and product contents and format. A brief review of the data quality is also given. Note that the focus of this manual are the Level-2 Land Surface Temperature and Fire Radiative Power products, and therefore the sections run in reverse order, with Level-2 described before Level-1.

Lastly, a Helpdesk section provides useful practical information, such as how to access and visualize the products. This section includes a list of frequently asked questions (FAQ) and useful links and references for more details about the SLSTR products.

2 SLSTR Land Quick Start

SLSTR is a dual view scanning radiometer, with 9 spectral bands (see Section 4.1), flying on the Sentinel-3A and Sentinel-3B satellites.

SLSTR land products provide three types of measurement described in this document:

- Level-2 **LST**: Land surface temperature maps (Section 6.2.1)
- Level-2 **FRP**: Fire radiative power products (Section 6.2.2)
- Level-1 **RBT**: Top of atmosphere radiance (mW/m^2/sr/nm) or brightness temperature (K) maps (Section 0)

Products are supplied in NetCDF-4 format in 3 minute 'granules' (see Section 6).

These products can be downloaded from the **ESA Copernicus Open Access Hub** (https://scihub.copernicus.eu), either searching by observation time, or by area of the globe (see Section 8.1.1). The global revisit time at the equator is less than one day when combining both satellites (see Section 3.3).

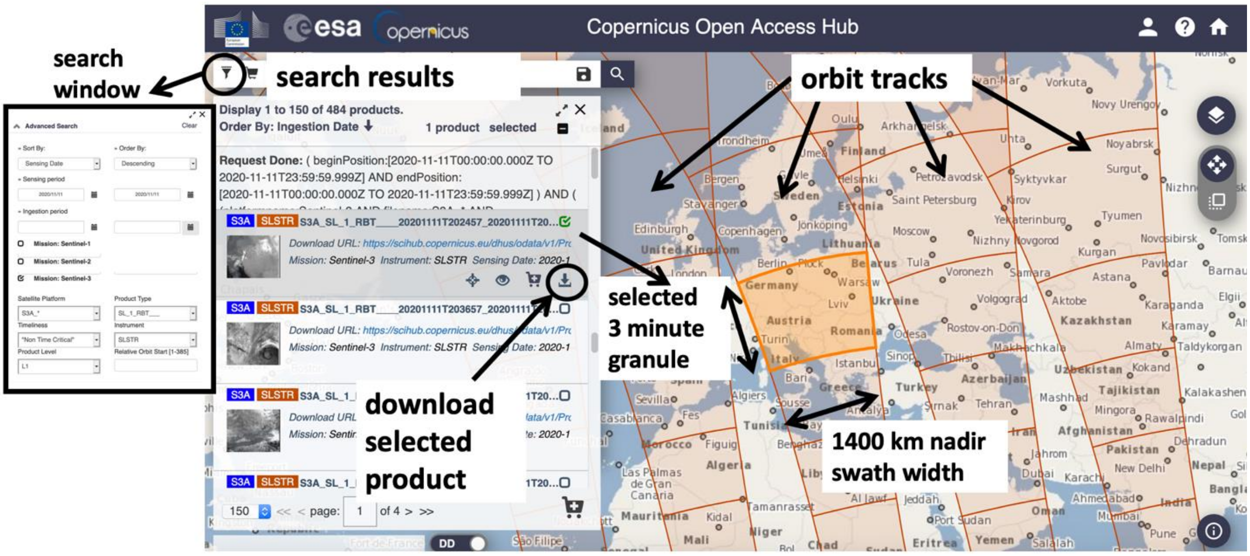

Once products are downloaded, they can be read, displayed and analysed using:

- The **ESA SNAP toolbox** (see Section 8.1.2)
- Other generic NetCDF tools, e.g. the **NASA Panoply tool**
- Standard Unix command, **ncdump** (ncdump -h to view the header only)
- Scripting languages, e.g. using the **Python netCDF4 library**

Land surface temperature products

- The **SL_2_LST** product contains LST from the SLSTR instrument at a spatial resolution of 1 km calculated using a split-window approach (Section 5.1.1).
- Validation (Section 7.3) provides evidence the product meets the mission requirements of being accurate to 1 K.
- LST data is only acquired for land (including permanent ice over land) and inland water. No LST data is available over open ocean pixels. The data have been quality checked with regards to input Level-1 data, with only valid data processed. All invalid data are identified with an exception flag.
- With respect to utilisation of LST of best quality it is recommended to apply the probabilistic cloud mask ('single_moderate' bit in the Bayes variable of the Flags datafile); this incorporates our best current knowledge of cloud contamination for SLSTR over land, ice and inland water pixels.

Fire radiative power products

The **SL_2_FRP** product contains two categories of data (Section 6.2.2):

- A LIST dataset providing information only for the granule pixels believed to contain actively burning fires. The LIST dataset contains a series of parameters for each of these active fire (AF) pixels, including their location, fire radiative power (FRP in MW) and FRP uncertainty (MW). Each parameter in the LIST dataset is stored as a 1D array of data, representing the value of that parameter for each of the detected AF pixels.
- A SUMMARY FLAG dataset providing information on every pixel in the granule, related primarily to the output of the active fire detection tests. These SUMMARY FLAG data are stored as a 2D array bit mask, and are typically significantly larger than the LIST dataset since they provide information everywhere in the granule and not just as the locations of detected AF pixels.

Many users will only require the information contained in the LIST dataset. However, those who want to understand why pixels were not identified as being an AF might want to inspect the SUMMARY FLAG dataset. For example, to identify which pixels were classed as cloudy and which as cloud free (since AF pixels can only be identified in pixels that were not masked as cloudy).

Level-1 radiance and brightness temperature products

The **SL_1_RBT** products contain top of atmosphere brightness temperatures (thermal infrared) and radiances (visible and shortwave infrared):

- Brightness temperatures (BTs) are mapped to a 1 km grid (thermal infrared) and radiances to a 500 m grid (visible and shortwave infrared) using a nearest neighbour algorithm (Section 0).
- BTs are accurate to within 0.1 K over the range 240 K to 320 K (Section 7.1.1).
- The geometric accuracy is within 50 m in nadir view along- and across-track and in oblique view across-track, and within 100 m in oblique view along-track (Section 7.2).

3 General information

3.1 The Copernicus Programme

Copernicus has been specifically designed in response to user requirements for environmental monitoring. Based on satellite and in-situ observations, the Copernicus services deliver near-real-time data on a global level which can also be used for local and regional needs, to help us better understand our planet and sustainably manage the environment we live in.

Copernicus is served by a set of dedicated satellites (the Sentinels) and contributing missions (existing commercial and public satellites). The Sentinel satellites are specifically designed to meet the needs of the Copernicus services and their users. Since the launch of Sentinel-1A in 2014, the European Union set in motion a process to place a constellation of almost 20 more satellites in orbit before 2030.

Copernicus also collects information from in-situ systems such as ground stations, which deliver data acquired by a multitude of sensors on the ground, at sea or in the air.

There are six Copernicus services whose aim is to transform the satellite and in-situ data into value-added information by processing and analysing the data. These services are: atmosphere, marine, land, climate change, security, emergency. The information provided by the Copernicus services can be used by end users for a wide range of applications in a variety of areas. The main users of Copernicus services are policymakers and public authorities who need the information to develop environmental legislation and policies or to take critical decisions in the event of an emergency, such as a natural disaster or a humanitarian crisis.

The Copernicus programme is coordinated and managed by the European Commission. The development of the observation infrastructure is performed under the aegis of the European Space Agency for the space component and of the European Environment Agency and the Member States for the in-situ component.

3.2 The European Space Agency

The European Space Agency (ESA) is dedicated to the peaceful exploration and use of space for the benefit of everyone. Established in 1975, ESA is an international organisation with 22 Member States and, for more than 40 years, has promoted European scientific and industrial interests in space. By coordinating the financial and intellectual resources of its members, it can undertake programmes and activities far beyond the scope of any single European country.

ESA's programmes are designed to find out more about Earth, its immediate space environment, our Solar System and the Universe, as well as to develop satellite-based technologies and services, and to promote European industries. ESA also works closely with space organisations outside Europe.

ESA's purpose shall be to provide for, and to promote, for exclusively peaceful purposes, cooperation among European States in space research and technology and their space applications, with a view to their being used for scientific purposes and for operational space applications systems:

- by elaborating and implementing a long-term European space policy, by recommending space objectives to the Member States, and by concerting the policies of the Member States with respect to other national and international organisations and institutions;
- by elaborating and implementing activities and programmes in the space field;
- by coordinating the European space programme and national programmes, and by integrating the latter progressively and as completely as possible into the European space programme, in particular as regards the development of applications satellites;
- by elaborating and implementing the industrial policy appropriate to its programme and by recommending a coherent industrial policy to the Member States.

The ESA Member States are: Austria, Belgium, Czech Republic, Denmark, Estonia, Finland, France, Germany, Greece, Hungary, Ireland, Italy, Luxembourg, the Netherlands, Norway, Poland, Portugal, Romania, Spain, Sweden, Switzerland and the United Kingdom. Slovenia and Latvia are Associate Members. Canada takes part in some projects under a cooperation agreement. Bulgaria, Croatia, Cyprus, Malta, Lithuania and Slovakia have cooperation agreements with ESA.

The budget of ESA for 2019 is €5.72 billion. ESA operates on the basis of geographical return, i.e. it invests in each Member State, through industrial contracts for space programmes, an amount more or less equivalent to each country's contribution.

ESA is developing a new family of missions called Sentinels specifically for the operational needs of the Copernicus programme. Each Sentinel mission is based on a constellation of (at least) two satellites to fulfil revisit and coverage requirements, providing robust datasets for Copernicus Services. These missions carry a range of technologies, such as radar and multi-spectral imaging instruments for land, ocean and atmospheric monitoring.

Looking to the future, six high-priority candidate missions are being studied to address EU policy and gaps in Copernicus user needs, and to expand the current capabilities of the Copernicus space component: CHIME – Copernicus Hyperspectral Imaging Mission, CIMR – Copernicus Imaging Microwave Radiometer, CO2M – Copernicus Anthropogenic Carbon Dioxide Monitoring, CRISTAL – Copernicus Polar Ice and Snow Topography Altimeter, LSTM – Copernicus Land Surface Temperature Monitoring, ROSE-L – L-band Synthetic Aperture Radar.

3.3 The Sentinel-3 mission

The Sentinel-3 mission is jointly operated by ESA and EUMETSAT to deliver operational ocean and land observation services. The main objective of the Sentinel-3 mission is to measure sea surface topography, sea and land surface temperature, and ocean and land surface colour with high accuracy and reliability to support ocean forecasting systems, environmental monitoring and climate monitoring. The mission definition was driven by the need for continuity in provision of ERS, ENVISAT and SPOT vegetation data, with improvements in instrument performance and coverage.

Sentinel-3A was launched on 16 February 2016 and Sentinel-3B was launched on 25 April 2018.

The spacecraft carries four main instruments:

- OLCI: Ocean and Land Colour Instrument
- SLSTR: Sea and Land Surface Temperature Instrument
- SRAL: SAR Radar Altimeter
- MWR: Microwave Radiometer
- These are complemented by three instruments for Precise Orbit Determination (POD):
    - DORIS: a Doppler Orbit Radio positioning system
    - GNSS: a GPS receiver, providing precise orbit determination and tracking multiple satellites simultaneously
    - LRR: to accurately locate the satellite in orbit using a Laser Retro-Reflector system.

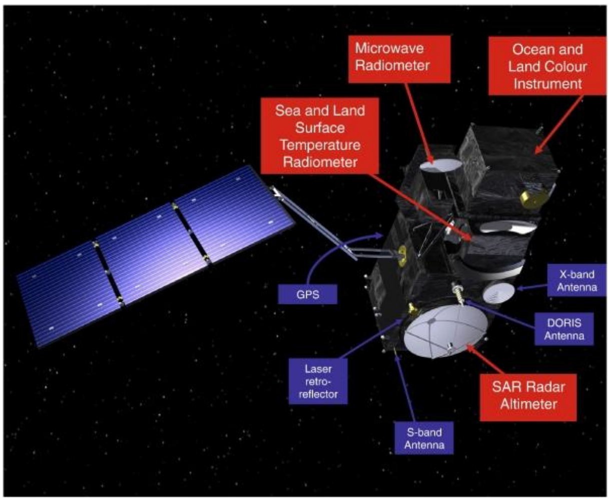

The Sentinel-3 orbit is similar to the orbit of Envisat allowing continuation of the ERS/Envisat time series. It uses a high inclination orbit (98.65°) for optimal coverage of ice and snow parameters in high latitudes.

The Sentinel-3 orbit is a near-polar, sun-synchronous orbit with a descending node equatorial crossing at 10:00 h Mean Local Solar time. In a sun-synchronous orbit, the surface is always illuminated at the same sun angle. The orbit reference altitude is 814.5 km.

The orbital cycle is 27 days (14+7/27 orbits per day, 385 orbits per cycle). The orbit cycle is the time taken for the satellite to pass over the same geographical point on the ground.

The two in-orbit Sentinel-3 satellites enable a short revisit time of less than two days for OLCI and less than one day for SLSTR at the equator based on the instruments' respective swath widths.

Sentinel-3B's orbit is identical to Sentinel-3A's orbit but flies +/-140° out of phase with Sentinel-3A.

4 SLSTR acquisitions

4.1 SLSTR instrument specifics

SLSTR is a scanning radiometer that is designed to provide accurate measurements of surface temperatures. The key features of SLSTR are:

- Thermal infrared (TIR) spectral bands at 3.74 µm, 10.8 µm and 12 µm with detectors that are cooled to 87K
- Channels in the Visible (VIS) to Short Wave InfraRed (SWIR) range for improved daytime cloud detection
- A dual view that allows the same terrestrial scene to be viewed through two atmospheric paths: a near nadir view, and an oblique view at 55° zenith angle.
- Two conical scanners to provide a 1400 km wide nadir view and 750 km oblique view.
- Two black-body sources, that are viewed by the scanners every scan cycle, provide continuous calibration of the infrared channels.
- A diffuser based VISible CALibration system (VISCAL) for calibrating the solar reflectance bands.

The spectral bands and their applications are listed in Table 1. A more detailed description of the SLSTR design and the predicted performance is described in Coppo et al. (2010).

Table 1: SLSTR Spectral Bands.

Band	Central Wavelength	Bandwidth	Spatial Resolution at Nadir	Function
S1	0.555 µm	0.020 µm	0.5 km	Chlorophyll, dual-view AOD over land
S2	0.659 µm	0.020 µm	0.5 km	Vegetation Index, dual-view AOD over land, masking of sunglint and clouds for daytime active fire detection
S3	0.870 µm	0.020 µm	0.5 km	Vegetation Index, dual-view AOD over land
S4	1.375 µm	0.015 µm	0.5 km	Thin Cirrus Cloud Detection
S5	1.610 µm	0.060 µm	0.5 km	Clouds, Active Fire (at night as alternative to S6), Ice/cloud discrimination
S6	2.225 µm	0.050 µm	0.5 km	Clouds, Active Fire (at night)

Band	Central Wavelength	Bandwidth	Spatial Resolution at Nadir	Function
S7	3.700 µm	0.380 µm	1.0 km	Night-time dual-view SST, Active Fire
S8	10.850 µm	0.900 µm	1.0 km	Dual-view SST/LST, Active Fire
S9	12.000 µm	1.000 µm	1.0 km	Dual-view SST/LST
F1	3.700 µm	0.380 µm	1.0 km	Active Fire
F2	12.000 µm	0.900 µm	1.0 km	Active Fire (not currently used)

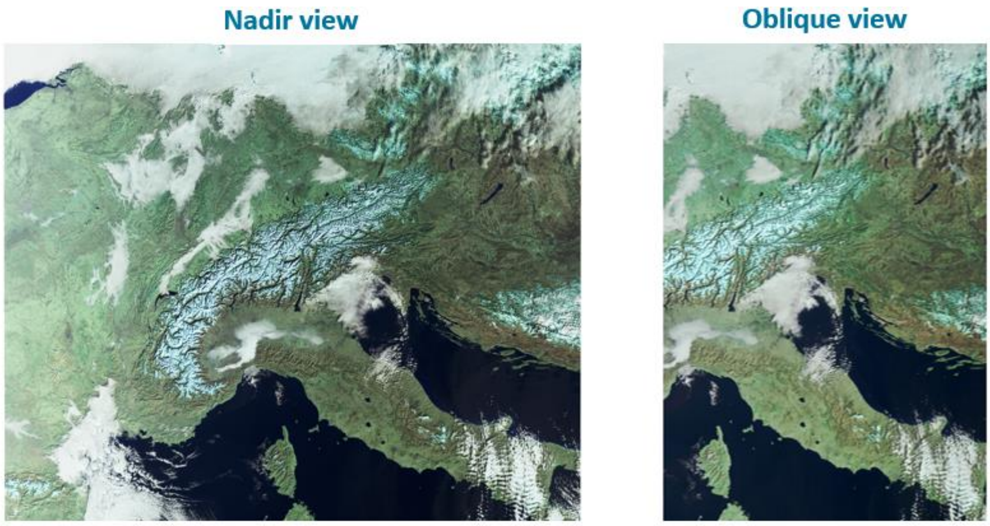

Figure 1: Example SLSTR image showing the nadir and oblique views.

4.2 Land measurement principles

4.2.1 Land Surface Temperature

The Land Surface Temperature (LST) is a measure of how hot or cold the 'surface' of the Earth would feel to the touch. It is the mean radiative temperature of all objects comprising the surface, as measured by ground-based, airborne, and spaceborne remote sensing instruments. The constituents of the Earth's surface (e.g. soil, vegetation, water, snow) vary from location to location. For each constituent, the LST is related to the points of maximum emission of electromagnetic radiation. Examples are bare soil and thick forest canopy which represent clear cases of this.

For bare soil and water, the skin depth is the important factor. The skin is defined as a layer of thickness equal to the penetration depth of the electromagnetic radiation and varies with the wavelength of the radiation and the nature of the material. The skin depth for a material is different at different wavelengths and also varies with surface conditions (such as degree of soil wetness, roughness) and view angle. At infrared (IR) wavelengths the soil skin depth is a few microns. For a dense forest with a closed canopy the skin temperature will be that of the forest canopy and is close to that of the air temperature at the top of the canopy. For more open vegetation the skin temperature will be an aggregation of all surface types within the field of view: soil and/or bare rock, vegetation and, if present, water or snow.

The LST determines the amount of energy emitted by the Earth's surface and is therefore a major factor in determining heat and water fluxes from the Earth's surface to the atmosphere. As applications for thermal infrared satellite imagery over land have increased so have the demands for these data to be of good quality. The SLSTR instrument observes with a spatial resolution of 1 km at nadir. These observations have high radiometric accuracy and are very well calibrated allowing for high quality LST data to be derived from them (Section 7).

4.2.2 Fire Radiative Power

SLSTR data are used to generate a Level-2 product (SL_2_FRP) related to biomass burning, and specifically to the location, timing and strength (in terms of fire radiative power output) of actively burning fires that were alight at the time of the satellite overpass. Background information on this type of 'active fire product' and detail on the SLSTR product in particular can be found in (Wooster et al., 2012 and Xu et al., 2020).

The requirement for satellite active fire (AF) products is driven by the fact that biomass burning is a key process shaping the Earth system, affecting the terrestrial biosphere and atmosphere through the combustion of vegetation and organic soils ('fuel'), transferring the vast bulk of their chemical constituents into the troposphere in the form of smoke (Figure 2a). Whilst landscape fires are a natural part of many ecosystems, human activity can greatly change fire regimes and can, for example, contribute to increasing atmospheric CO_2 concentrations through deforestation, tropical peatland burning, and via areas seeing an increase in their fire return interval. In this and other ways, landscape fires impact radiative forcing, and in addition to CO_2 also release the strong greenhouse gas methane (Nguyen & Wooster, 2020). They are furthermore a major source of aerosols, CO and oxides of nitrogen to the atmosphere, with the ability to greatly affect air quality at distances even far away from the fires themselves. Satellite remote sensing is the only way to provide globally consistent information on landscape fire activity, and estimates of the magnitude of landscape fires and fire emissions are required for realistic modelling of a number of Earth system processes, including the global carbon cycle and climate, and also for air quality early warning and many landscape and fire management purposes.

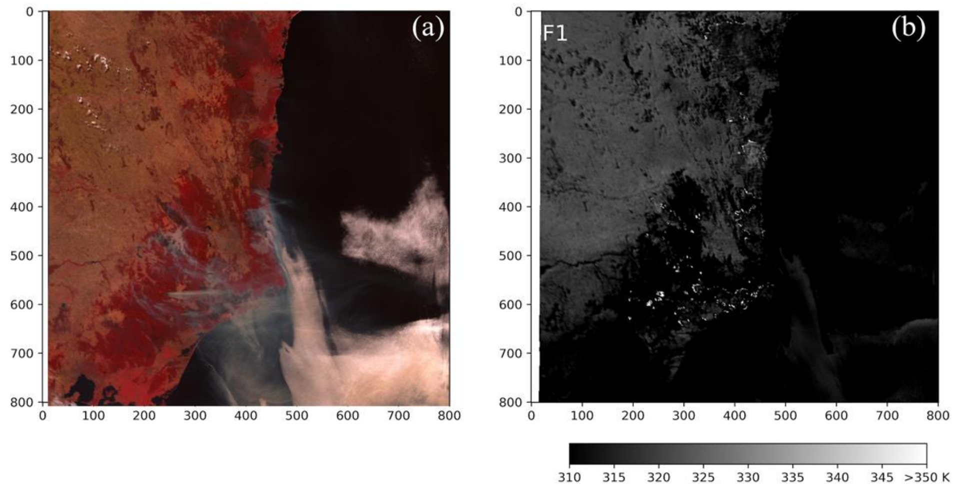

Figure 2: Example of a large wildfire burning in Australia as observed in the SLSTR Level-1 data from the near-nadir view at 23:08 UTC on 3 Jan 2020. (a) False colour composite composed of data from the S3, S2 and S1 channels where smoke plumes from the fires can be seen, and (b) F1 channel data where pixels containing actively burning fires appear bright due to their elevated brightness temperatures.

When biomass is burned it releases an approximately fixed amount of thermal energy per kg consumed, some of which is released as (primarily infrared) electromagnetic radiation. Remotely sensed measurements of this electromagnetic radiation - such as those provided by SLSTR - can be used to identify the presence of an actively burning fire within a pixel, even though the fire itself may cover less than 1% of the pixel area (see explanation for this sensitivity in Wooster et al., 2003). The middle infrared (MIR) bands of SLSTR are the most sensitive to the presence of actively burning fires, and the bright pixels of Figure 2b shows where fires are burning at the time the image was taken, data that forms the basis of the active fire detection process.

Estimates of the rate of thermal energy emission from detected active fire pixels - the so called Fire Radiative Power (FRP) - can then provide information useful for estimating the rate of fuel consumption and the rate of emission to the atmosphere of carbon and the various chemical compounds present within smoke (see Nguyen & Wooster, 2020). Because of this importance, Fire Disturbance (including AF detection and FRP assessment) has been identified as an Essential Climate Variable (ECV) by the Global Climate Observing System (Sessa, 2008), and the Sentinel-3 FRP product has been explicitly designed to provide this information.

Landscape fire activity is present in most vegetated environments, and global data obtained via satellite Earth Observation is required for its quantification. SLSTR provides information on landscape fire activity in the morning and evening, at overpass times similar (but not identical to) those of the MODIS instrument that has operated onboard the Terra satellite since 2000. An example of global SLSTR active fire detections (AF pixel counts) made by S3B during January 2019 is shown in Figure 3. Landscape fire is a highly dynamic phenomena, with the ability to change considerably from one hour to the next and which typically shows a very strong diurnal variability. Fire activity generally peaks in the early afternoon in most regions of the planet, with a minimum at night (Giglio, 2007; Roberts et al., 2009).

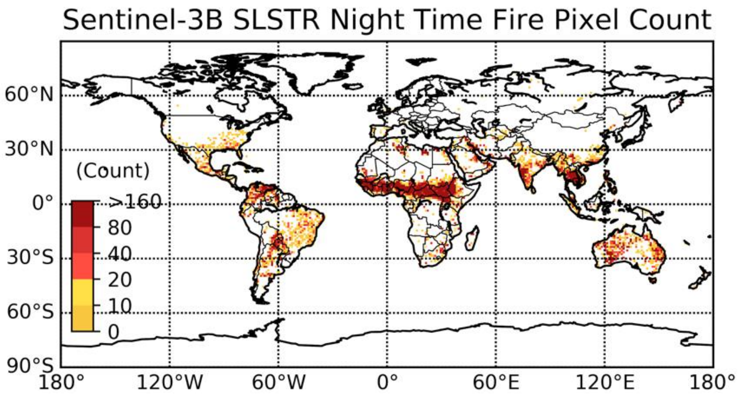

Figure 3: Global map of night time active fire pixel counts present in the Sentinel-3B SLSTR Level-2 FRP products from January 2019. Active fire counts are presented as the monthly total detected in 1 degree grid cells. Fire activity is seasonal, so for example far more AF counts would be expected in e.g. Southern hemisphere Africa in later months of 2019.

The data contained within the Sentinel-3 FRP product is similar in nature to that provided by MODIS Terra and is collected at a similar time of day - so ultimately it will take over from this source to continue to produce a globally consistent record. At present the Sentinel-3 FRP product delivers information primarily from the satellites night-time (ascending node) passes (S3 satellite equatorial crossing time of 22:00 hrs), with daytime data from the 10:00 hrs equatorial crossing time only produced in areas where the SLSTR S7 channel remains unsaturated over the ambient land surface (the S7 channel saturates above a signal of around 311 K). A full daytime version of the FRP product algorithm and the resulting full daytime version of the FRP product will be developed in the coming period. In terms of the night-time AF detections, early evidence indicates that when the Level-2 SLSTR FRP product and MODIS Terra AF products are produced for the same area near simultaneously, the SLSTR product tends to detect more active fire pixels (see Section 7.4). However, the FRP total from the near-simultaneously observed regions appear to be very similar for SLSTR and MODIS Terra since the additional AF pixels detected by SLSTR tend mostly to be associated with low FRP fires.

4.3 Calibration and Validation

4.3.1 Thermal Infrared Channels

SLSTR is designed to be self-calibrated via two on-board cavity black-body (BB) sources. One BB is heated to ~302 K by applying a constant power to the cavity baffle and base, while the other ‘floats’ at the instrument temperature (nominally 250-270 K). The two blackbodies are positioned ahead of the complete SLSTR optical chain, and are viewed every 0.6 s scan cycle. The conical scan geometry ensures that the signals from the BBs enter the SLSTR optics at the same low angle of incidence as the Earth scene so no corrections for view angle or polarisation are necessary. Also, because the calibration sources are viewed every scan, no special calibration modes are needed ensuring continuous acquisition of Earth scene data.

The radiances of the black-bodies are derived via the Planck radiation law from their physical temperatures which are measured by precision platinum resistance thermometers (PRTs). These were calibrated in situ before launch against Standard PRTs to provide traceability to the International-Temperature-Scale of 1990.

Before launch, the instruments underwent a thorough calibration campaign under flight representative thermal vacuum conditions to verify the end-to-end calibration (Smith et al., 2020).

4.3.2 Visible/Short Wave Infrared Channels

The visible/SWIR channels are calibrated via two on-board reference sources. A diffuser based VISible CALibration source (VISCAL) is illuminated once per orbit by the Sun to provide an upper calibration reference source (Coppo et al., 2010). The dark signal (offset) is measured continuously during the orbit using one of the on-board BB sources.

5 SLSTR Algorithms and Processing levels

SLSTR data are measured in the instrument geometry relative to the scanning mirror position, detector readouts and motion of the satellite (the 'instrument frame'). These data are processed to useable images and products by the operational processor over three stages (in reverse order):

- **Level-2**: This stage applies a retrieval algorithm to process the Level-1 data and deliver final geophysical products, such as land surface temperatures and information on actively burning fires. At this stage, the processor is divided into a 'Land' branch under the responsibility of ESA (land surface temperature, fire radiative power), and a 'Marine' branch (sea surface temperature) under the responsibility of EUMETSAT.
- **Level-1**: This stage of the processing produces geo-located radiometric measurements for each SLSTR channel/view. It is common to Land and Marine branches.
- **Level-0**: This stage of the processing formats the stream of instrument source packets into raw data products – these are for internal use only and are not disseminated to users.

5.1 Level-2

5.1.1 Land Surface Temperature

The Sentinel-3 processing chain delivers LST and its associated uncertainty as core Level-2 operational product. It further provides auxiliary information that has been used for the LST retrieval, such as land cover type, fractional vegetation cover, total column water vapour, normalized difference vegetation index (NDVI), and quality control flags. The purpose of making these data available is to give the user maximum flexibility in selecting data for their application.

The Sentinel-3 Level-2 SLSTR LST algorithm (see the *LST ATBD*) uses a nadir-only split-window approach (Ghent et al., 2017). Split-window algorithms correct for atmospheric effects using the differential absorption in two (or more) IR bands within the same atmospheric window (band of relatively high atmospheric transmittance). In the case of Sentinel-3 the algorithm uses the S8 and S9 channels for the nadir view.

The LST is estimated as a combination of calculated coefficients and observed brightness temperatures (BT). The coefficients are derived by regressing BTs, simulated with a radiative transfer model for a realistic range of atmospheric conditions, against the model input skin temperatures. The classes of coefficients applied to the algorithm are dependent on the biome, fractional vegetation cover and water vapour for each combination of biome-diurnal (day/night) condition. The fractional vegetation cover and water vapour are seasonally dependent whereas the biome is invariant. Land surface emissivity (LSE) is implicitly handled within the fractional vegetation dependent retrieval coefficients.

The biome auxiliary data is a variant of the Globcover classification (Arino et al., 2007) re-gridded to 1/120°. To capture the emissivity variability for bare soil regions the original Globcover bare soil class has been divided into six separate classes, taking the total number of land and inland water classes to 27. Table 2 describes the 27 biome classes. Fractional vegetation cover is based on the Copernicus Global

Land Service FCOVER dataset, which is available globally at the desired near 1-km resolution of 1/112° (Baret et al., 2013). Water vapour is derived from the European Centre for Medium-Range Weather Forecasts (ECMWF) ERA-Interim reanalysis (Dee et al., 2011). Each auxiliary data file (ADF) is derived from 6-hourly monthly climatology corresponding to the 4 synoptic times - 00UTC, 06UTC, 12UTC and 18UTC. Snow masking is derived, in the Northern hemisphere, from daily maps created by the Interactive Multisensor Snow and Ice Mapping System (IMS). In Southern hemisphere, snow masking is based on the [Istomina and all, 2010] and [Eastwood and Andersen, 2007] approaches.

Table 2: Description of the 27 land and inland water biomes used in the LST retrieval. The Open ocean biome relates to any pixel not processed for LST.

Numeric Code	Text Code	GlobCover legend
0	Open ocean	Open ocean
11	Irrigated cropland	Post flooding or irrigated croplands
20	Rain-fed cropland	Rainfed croplands
30	Mosaic vegetation	Mosaic cropland (50-70%)/vegetation (grassland, shrubland, forest) (20-50%)
40	Broadleaved evergreen forest	Closed to open (<15%) broadleave evergreen and/or semi-deciduous forest (>5m)
50	Closed broadleaved deciduous forest	Closed (>40%) broadleaved deciduous forest (>5 m)
60	Open broadleaved deciduous forest	Open (15-40%) broadleaved deciduous forest (>5 m)
70	Closed needleleaved forest	Closed (>40%) needleleaved evergreen forest (<5 m)
90	Open needleaved forest	Open (15-40%) needleleaved deciduous or evergreen forest (<5 m)
100	Mixed forest	Closed to open (>15%) mixed leave broadleaved and needleleaved forest (<5 m)
110	Mosaic forest	Mosaic forest/shrubland (50-70%) / Grassland (20-50%)
120	Mosaic grasslands	Mosaic grassland (50-70%) / Forest / Shrubland (20-50%)
130	Shrubland	Closed to open (>15%) shrubland (<5m)
140	Grassland	Closed to open (>15%) grassland
150	Sparse vegetation	Sparse (>15%) vegetation (woody vegetation, shrubs, grassland)
160	Freshwater flooded forest	Closed (>40%) broadleaved forest regularly flooded - fresh water
170	Saltwater flooded forest	Closed (>40%) broadleaved semi-deciduous and /or evergreen forest regularly flooded - saline water
180	Flooded vegetation	Closed to open (>15%) vegetation (grassland, shrubland woody vegetation) on regularly flooded or waterlogged soil - fresh, brackish

Numeric Code	Text Code	GlobCover legend
		or saline water
190	Artificial surface	Artificial surfaces and associated areas (urban areas > 50%)
200	Bare area	Bare areas
210	Water	Inland water bodies and coastal water
220	Snow and ice	Permanent snow and ice
230	No data	No data (burnt areas, clouds...)

The LST observations have an associated uncertainty estimate, since effects such as atmospheric attenuation and variability of surface emissivities are not known to suffcient accuracy; and the appropriate estimation of these uncertainties a necessary accompanying information in the product. The SLSTR LST uncertainty model follows an established methodology in the LST community whereby for each pixel different components of uncertainty are provided, representing the uncertainty from effects whose errors have distinct correlation properties: random (no correlation of error component between cells); locally systematic (correlation of error component between 'nearby' pixels); large-scale systematic (correlation of error component between 'distant' pixels). Since all effects can be treated independently, the total uncertainty per pixel is acquired by adding all the components in quadrature. The different components are visualized in Figure 4.

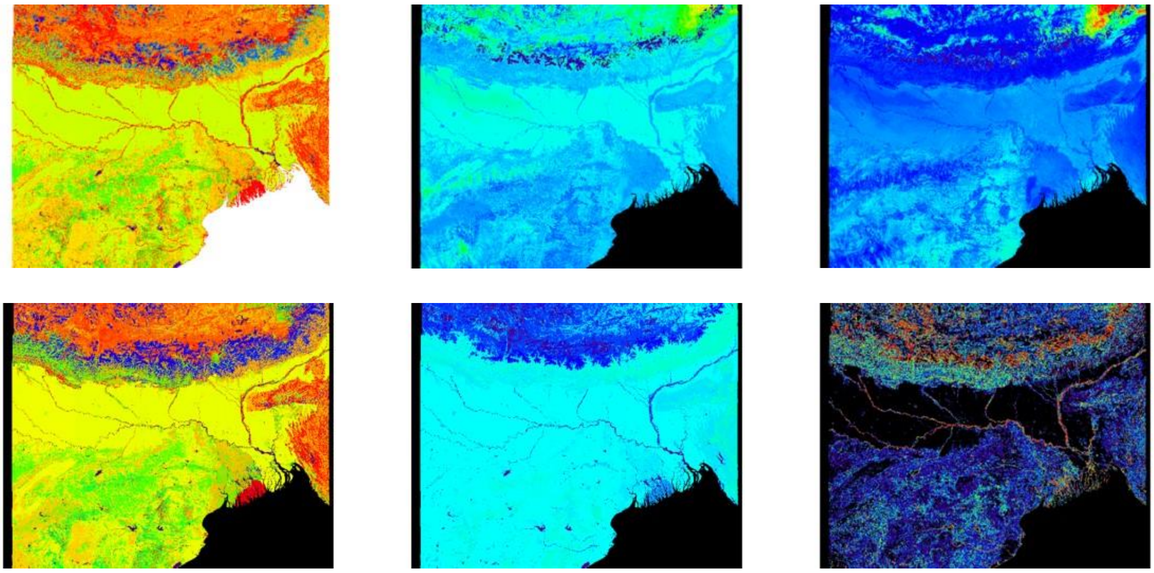

Figure 4: Example of the per-pixel LST uncertainty model components: total uncertainty (top-left); random uncertainty (top-centre); calibration uncertainty (top-right); locally correlated atmosphere uncertainty (bottom-left); locally correlated surface uncertainty (bottom-centre); and locally correlated geolocation uncertainty (bottom-right).

5.1.2 Fire Radiative Power

The processing chain that delivers the Sentinel-3 SLSTR Level-2 FRP product is based on (i) the detection of SLSTR pixels in the near nadir view believed to contain actively burning fires, and (ii) the per-pixel retrieval of FRP at each of these confirmed AF pixels. Figure 3 showed an example of the AF pixel counts detected in January 2019 from Sentinel-3B, gridded at 1 degree globally. Data from the SLSTR oblique view are unused for the FRP product generation, since this offers a narrower swath and a coarser pixel size compared to the near nadir view. Specifically to support the generation of these AF products, the SLSTR instrument possesses a low-gain channel in the middle infrared spectral region that is able to measure brightness temperatures in excess of 450 K (the F1 channel, Table 1).

To generate the SLSTR FRP product, pixels in the near nadir view are first masked for cloud cover using a set of simple thresholding tests developed specifically for the active fire application (Wooster et al., 2012; Xu et al., 2020). AF pixels cannot be detected through thick meteorological cloud, and indeed clouds can in some circumstances be the cause of 'false alarm' AF detections[1], so cloud masking is important. However, the cloud mask from the Level-1 product file is not used to generate the Level-2 FRP product since it has been optimised for other (non-fire) applications, leading to it possibly masking out slightly cloud-contamined areas where AF detection might still be possible. The other key mask applied in the FRP product algorithm is a sunlgint mask, again to avoid (daytime) false alarms. Whilst vegetation fires can only burn on land, masking of all oceanic areas is not conducted because the detection of offshore gas flares is also of interest.

All non-masked pixels in the granule are then tested to see if they seem likely to contain actively burning fires at the time they were observed. This testing is conducted using a contextual AF detection algorithm, based on the kinds of principles applied when generating the MODIS AF products (Giglio et al., 2003). The SLSTR AF detection and FRP retrieval algorithm was developed prior to the Sentinel-3A launch by Wooster et al. (2012), and substantially modified and optimised post-launch by Xu et al. (2020). The contextual approach attempts to identify AF pixels via their radiometric contrast with their non-fire neighbours, with the aim of successfully detecting pixels that contain even low FRP fires whilst avoiding false alarms from such phenomena as cloud edges and, by day, sunglint. Observations in the middle infrared spectral region are key to this ability, and the SLSTR observations in the S7 and F1 channels (Figure 5), along with the contextual AF detection algorithm and information from various other spectral channels are extremely sensitive to the presence of fire. SLSTR pixels containing areas of combustion covering down to only around 10^{-3} to 10^{-4} of a pixel area can typically be successfully identified, and once identified the FRP of each confirmed AF pixel is then retrieved using the MIR radiance method of Wooster et al. (2003, 2005). The full algorithm used to generate the S3 FRP Products is detailed in the *FRP ATBD*, and also in the pre-launch algorithm definition detailed in Wooster et al. (2012) and its significant post-launch update Xu et al. (2020).

[1] These false alarms are due to the fact that clouds have a high MIR-TIR difference, like fires. If there is a small fraction of cloud within a land pixel, it can sometimes be miss-classified as a fire, especially at cloud edges where the temperature is higher than the middle of a normal cold cloud.

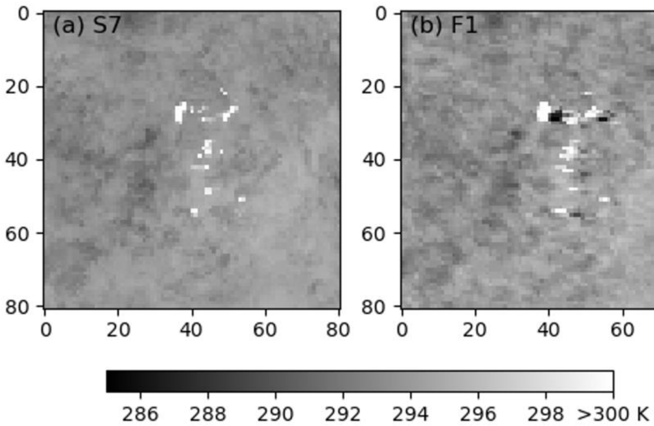

Figure 5: Example of a large wildfire observed with Level-1 SLSTR data from (a) the S7 channel, and (b) the F1 channel. Whilst the same fires are identified in both S7 and F1, the number of AF pixels in a fire cluster and the shape of the cluster are slightly different between S7 and F1 due to the different pixel footprint characteristics of the two channels. Also seen is the low brightness temperature anomaly (dark pixels) which affect F1 channel data downscan of high brightness temperature pixels.

Each Level-2 FRP product file contains information on the locations of the AF pixels burning at the time of the Sentinel-3 overpass, along with pixel-level information on their spectral signatures, FRP and FRP uncertainty (Section 6.2.2). Once the set of confirmed AF pixel detections are made, an atmospheric transmittance correction is applied to their retrieved FRP values to account for the effects of atmospheric attenuation. A complexity with SLSTR is the saturation of the S7 channel at relatively low temperatures, and data from this channel is not used in the Level-2 algorithm when it reports a brightness temperature above 311 K, which frequently happens at AF pixels and also over many ambient land surfaces by day. When this happens, data from the F1 channel are used instead of those from S7, though the slight geometric offset and different pixel shape between these two channels (see Section 7.7) introduces added complexity to the algorithm (see Xu et al., 2020). However, the F1 channel offers the advantage that its pixel size remains smaller and far more consistent across the swath than does that of S7, and this enables smaller and less intensely burning (i.e. lower FRP) fires to be detected than would otherwise be the case, particularly at locations towards the swath edge. To take advantage of this, in the Level-2 FRP product available on the Sentinel Data Hub, all AF pixels are ultimately detected and have their FRP retrieved using the F1 channel, subsequent to a first AF pixel detection step that is based on S7 (see Xu et al., 2020 for full details).

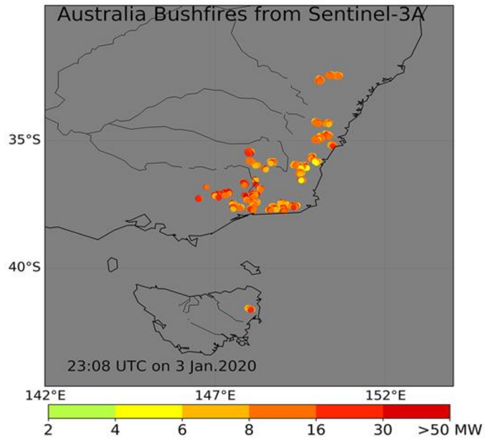

Figure 6: Graphic of the FRP retrievals made at the location of all active fire pixels detected in the S3A SLSTR Level-1 data of Australia shown in Figure 2 and stored in the corresponding Level-2 FRP product file.

Since February 2022, fires are also detected during nighttime using the SWIR S6 radiances. As these SWIR channel signals should essentially be very close to zero over ambient temperature surfaces during nighttime, fires are emitting significantly at these wavelengths. Any fire missed by the test based on the MIR and LWIR signals have another chance to be detected using these SWIR signals, especially thanks to the smaller 500m pixel size as any fire will comprise a higher proportion of SWIR pixel area. The detection is then based on a absolute test comparing SWIR S6 and S5 fire radiances and the mean and median SWIR channel radiances computed over a large neighbouring area.

5.2 Level-1

The purpose of Level-1 processing is to calibrate the raw instrument data, geo-locate each pixel to its position on the Earth, put the pixels on a uniform grid and add other auxiliary information (see the *L1 ATBD*).

Step 1: Read in the raw data. Important variables such as the raw counts, instrument temperatures, and pointing direction of the satellite are extracted for use in the following steps.

Step 2: Calculation of calibration parameters. The two BB calibration sources (see Section 4.3.1) are used to calculate the radiometric gain and offset parameters for the infrared channels (S7-S9, F1-F2). The visible/SWIR calibration parameters are calculated using the VISCAL system (see Section 4.3.2), which observes the Sun once every orbit.

Step 3: Geolocation. The exact location that the instrument is viewing on the surface of the Earth when each pixel was measured is calculated. This uses the satellite position, viewing angles, the 'line of sight' of each pixel within the instrument, and a digital elevation model of the Earth.

Step 4: Re-gridding. SLSTR observations are made in the 'instrument frame', measured in curved lines following motion of the conical scanner (see Figure 7). These measurement pixels are 're-gridded' onto a uniform quasi-Cartesian 'image grid', defined relative to the sub-satellite track which forms the 'y' axis. The y=0 position is the point that the satellite crosses the Equator at the ascending node (South to North). Each image grid pixel is a uniform 1km×1km (or 0.5×0.5km, depending on the channel). The image grid is filled with measurements using a nearest-neighbour algorithm. Note that the geographic centre of each measurement pixel is not necessarily the same as the geographic centre of the image grid pixel, nor is it always the same shape (see Figure 8). Due to the curved measurement scans, this approach can lead to some image pixels with no measurements, or with more than one measurement – the gaps are 'cosmetically filled' (see Section 8.2.12), and the additional samples are stored as 'orphans' (see Section 8.2.12).

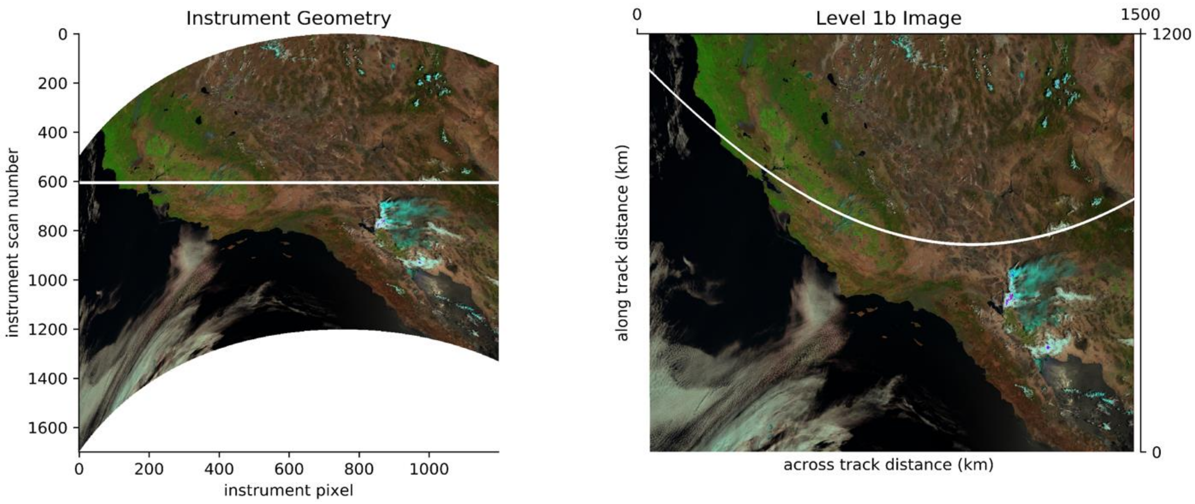

Figure 7: A nadir view image in instrument geometry (left) and after regridding onto the Level-1 image grid (right). The white line shows the path traced on the surface of the earth by a single detector during one scan of the instrument conical scanner.

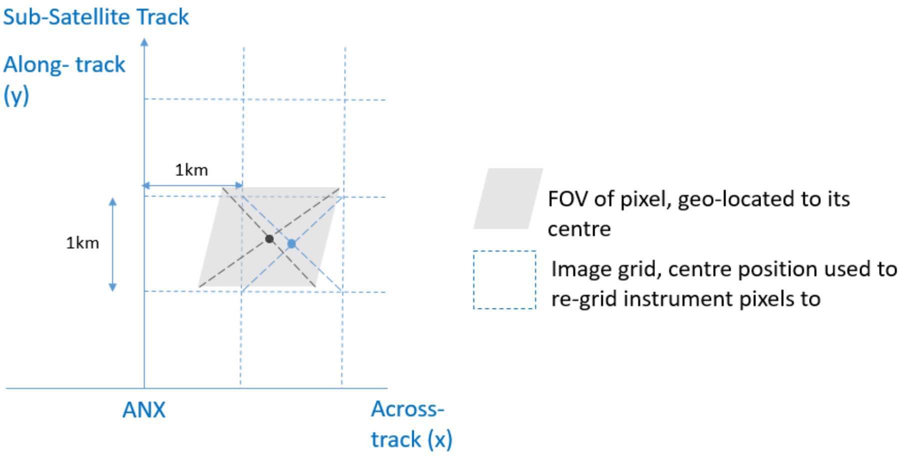

Figure 8: A diagram showing the definition of the 1km image grid. The x and y Cartesian coordinates are defined relative to the Ascending Node Crossing (ANX) and the sub-satellite track. This figure illustrates the difference between the image grid pixel, and the actual field of view of the instrument pixel. The 0.5km grids are referenced in a similar way.

Step 5: Cloud Masking and other classifications. Additional information is added such as surface classification, and each pixel is determined to be either clear or cloudy by a number of different cloud tests (see the *L1 ATBD*). Finally, Meteorological data fields taken from models near the time of SLSTR measurements are added to the product.

6 SLSTR products

6.1 Introduction to SLSTR land products

There are three SLSTR land product types distributed to users: **SL_1_RBT** (Level-1 radiances and brightness temperatures), **SL_2_LST** (Level-2 land surface temperature), and **SL_2_FRP** (Level-2 fire radiative power). The following sections describe these products in reverse order, starting with Level-2.

The product data for each type are saved in the Standard Archive Format for Europe (SAFE), which consists of an XML manifest (xfdumanifest.xml) and a set of measurement and annotation data files in Network Common Data Format (NetCDF-4). The manifest file gives summary information for the product, and is used for reading it into the SNAP toolbox. The NetCDF format is a platform independent, self-describing data format, containing data, metadata and descriptions. The collection of files for each SAFE product can exist as a directory in a filesystem, zipped folder or tarball depending on where the data were obtained.

Note that within the NetCDF files, some variables types (e.g. Level-1 radiance/BT) can be given with a scale factor and/or offset. This is taken into account automatically by some data readers, but must be applied manually if read by hand inside a script.

SLSTR products are uniquely defined by their ‘processing baseline’ configuration (see Section 8.2.2). This indicates both the software version and the internal auxiliary data files (ADFs) used to generate the product. When a significant change is made to the processing, the ‘**Baseline Collection**’ number is incremented - this number is contained in the filename (see below).

SLSTR products are divided into Product Dissemination Units (PDU), or granules, which contain a 3 minute portion of data. These product granules are delivered to users twice: firstly within 3 hours of acquisition (Near Real Time, or **NRT** data), and secondly more slowly once consolidated orbit and meteorological data are available (Non Time Critical, or **NTC** data). Typically the NTC data should be available within 24-48 hours of acquisition, and are recommended for the majority of non-operational users. In spite of slight differences in calibration, the absolute geolocation of each measurement position should be the same in both NRT and NTC products.

The filename convention for SLSTR products is summarised below:

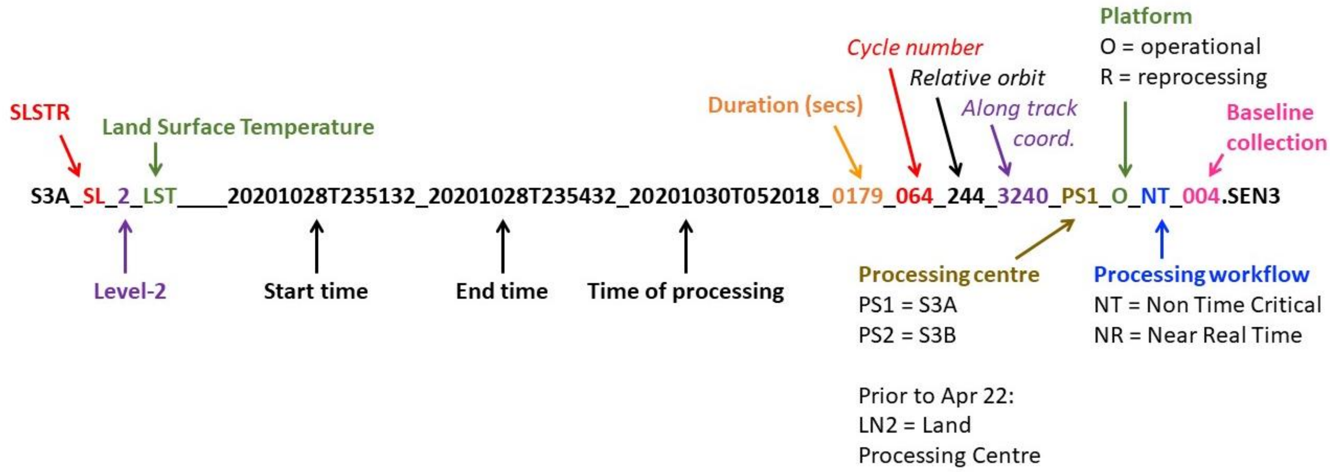

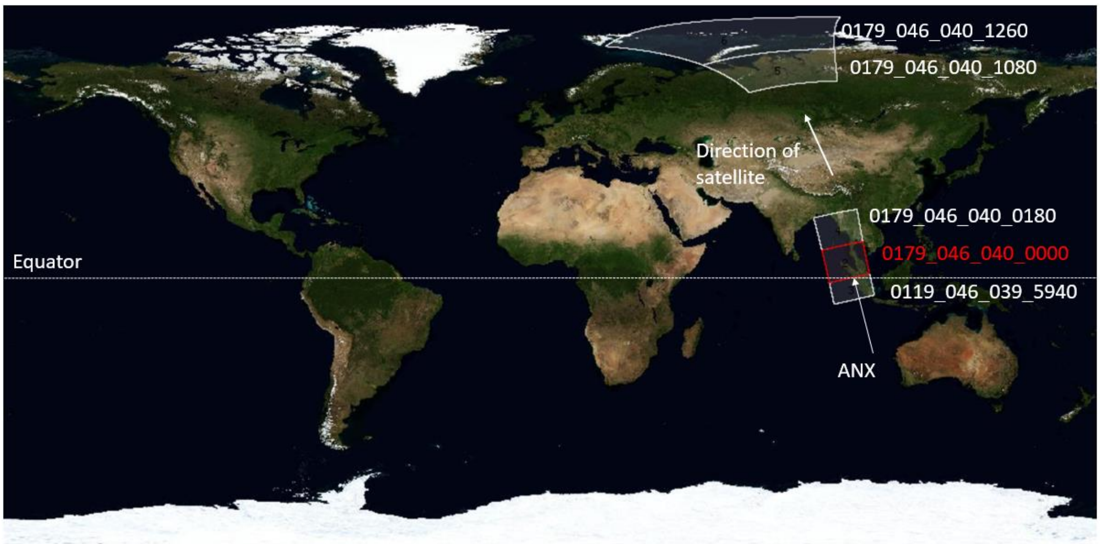

Figure 9: The location and extracts of filenames of a number of products from cycles 39 and 40 of relative orbit number 46 are shown on a global image. Note the shorter measurement time of the final product in the cycle, and how the along-track coordinate number starts from the ANX.

6.2 Level-2 product content

6.2.1 Land Surface Temperature

The SL_2_LST product is the core Level-2 product for Sentinel-3. For both NRT and NTC products the data is available in 3-minute PDUs (granules) generated from the input nadir S8 and S9 brightness temperatures in the Level-1 data.

Each product consists of an XML manifest file (xfdumanifest.xml) and a set of eleven measurement and annotation data files in NetCDF-4 format. These include data on both the image grid (*_i?.nc files) and tie-point grid (*_t?.nc files) – see also Section 0. Geophysical information is provided on the geolocation in both Cartesian (cartesian_*.nc) and Geodetic (geodetic_*.nc) forms; satellite and solar zenith and azimuth viewing angles (geometry_tn.nc); instrument level scan, pixel and detector origins (indices_in.nc); acquisition time (time_in.nc), but only when used in combination with the indices_in.nc data using the approach in Section 8.2.6; meteorological conditions (met_tx.nc); cloud masking (flags_in.nc); and the LST (LST_in.nc and LST_ancillary_ds.nc).

For straightforward use of the LST data the key datafile is the LST_in.nc. This contains the LST variable and the LST_uncertainty variable. The latter being the total uncertainty per pixel on the calculated LST, which is a combination of all the different components of uncertainty on the LST retrieval. The LST_ancillary_ds.nc datafile contains the various auxiliary data used within the split-window LST retrieval scheme (Section 5.1.1), such as TCWV (total column water vapour), biome, and fraction (fractional vegetation cover). It also contains the NDVI. Table 3 details these variables. A breakdown of the different components of the LST uncertainty is also available in the LST_ancillary_ds.nc datafile.

Table 3: Primary LST information in the two main Level-2 SLSTR LST product files: LST_in.nc (orange); LST_anillary_ds.nc (green). The dimensions are common to both. In addition to these variables on the image grid there are equivalent variables and an accompanying dimension for the orphan pixels.

Name	Type	Dimensions	Units	Comment
LST	short	rows, columns	K	land surface temperature
LST_uncertainty	short	rows, columns	K	total land surface temperature uncertainty
exception	short	rows, columns	unitless	quality control flags
biome	ubyte	rows, columns	untiless	land cover classification (biome) between 1 and 27
fraction	short	rows, columns	unitless	fractional vegetation cover between 0 and 1
TCWV	short	rows, columns	kg m^{-2}	total column water vapour
NDVI	short	rows, columns	unitless	normalised difference vegetation index

It is important to note that unlike the Level-1 data which is complete for the whole PDU, the LST data is limited to land (including permanent ice over land) and inland water only. Any pixels which are identified as sea are filled with the specified '_FillValue' (e.g. NaN) for each variable. The 'exception' field provides the quality control information for when LST is not produced for a pixel which is over land or inland water.

Table 4: Exception flags for the LST data.

Bit number	Text code	Description
0	ISP_absent	ISP absent
1	Pixel_absent	Pixel absent
2	Not_decompressed	Not decompressed
3	No_signal	No signal in channel
4	Saturation	Saturation in channel
5	Invalid_radiance	Derived radiance outside calibration
6	No_parameters	Calibration parameters unavailable
7	Unfilled_pixel	Unfilled pixel
8	LST_underflow	LST underflow
9	LST_overflow	LST overflow
10	biome	LST could not be calculated for this biome type

Of key importance for quality LST data is to ensure the data are appropriately cloud cleared. The LST variable in the LST_in.nc datafile contains LST that has not been cloud cleared. The user is provided with the necessary information to perform this task within the flags_in.nc datafile. This datafile contains variables describing the cloud masking, pointing and overall confidence, and are presented in Table 5.

Table 5: Flagging information in the Level-2 SLSTR LST product. In addition to these variables on the image grid there are equivalent variables and an accompanying dimension for the orphan pixels.

Name	Type	Dimensions	Units	Comment
cloud_in	ushort	rows, columns	unitless	threshold based cloud tests
bayes_in	ubyte	rows, columns	unitless	probabilistic cloud test
pointing_in	ubyte	rows, columns	unitless	pointing information
confidence_in	ushort	rows, columns	untiless	quality control flags including summary_cloud flag (based on probabilistic cloud test)

The 'cloud_in' variable contains the individual threshold tests which comprise the basic cloud test. The purpose of these tests are for generic cloud masking for any land products. In contrast, the probabilistic cloud test has been specifically designed for LST applications. This test is identified in bit 1 of the 'bayes_in' variable, and is labelled 'single_moderate'.

The Probabilistic cloud mask is based on the probability of clear-sky conditions, which is a semi-Bayesian approach. It uses atmospheric profile information to interpret clear-sky conditions for the coincident space and time of acquisition by the instrument. The coincidence is modelled through profiles direct from the meteorological fields in 'met_tx.nc' and temporal interpolation between 6-hourly analysis fields. Using a radiative transfer model, expected clear-sky brightness temperatures / brightness temperature differences (BTDs) are simulated for these profile data. Pixel information on clear-sky conditions within a granule are derived from probability density functions (pdf), in which a normal distribution is assumed. For each pdf, the mean is the simulated brightness temperature / BTD for the granule and the standard deviation is the observational climatology for the corresponding month, biome, and diurnal state. A per-pixel cloud mask is generated from comparing the pixel BTs /BTDs with the pixel pdfs. If the combined probabilities are less than a 99% confidence threshold of clear sky then the pixel is identified as cloudy. The Probabilistic cloud mask was previously derived and outputted by the Level-1 processing. This processing has been move to Level-2 LST processing chain in February 2022.

The 'confidence_in' variable contains quality information on the LST observation, and is detailed in Table 6. Note that the snow and sea-ice flag and the summary_cloud flag (now computed using only probabilistic flag) are the only ones not directly transferred from SLSTR L1b product but recomputed inside LST processing (see section 5.1.1).

Table 6: Quality flags for the LST data in the 'confidence_in' variable.

Bit number	Text code	Description
0	coastline	Coastline pixel
1	ocean	Ocean pixel
2	tidal	Tidal pixel
3	land	Land pixel
4	inland_water	Inland water pixel
5	unfilled	Unfilled pixel
6	spare	
7	spare	
8	cosmetic	Cosmetically filled pixel

Bit number	Text code	Description
9	duplicate	Duplicate pixel
10	day	day / night flag
11	twilight	Pixel is in twilight conditions
12	sun_glint	Pixel is subject to sun glint
13	snow	Pixel is snow covered
14	summary_cloud	Combination of the flags in the 'cloud_in' variable
15	summary_pointing	Combination of the flags in the 'pointing_in' variable

The main LST data and supporting variables are illustrated in an example in Figure 10.

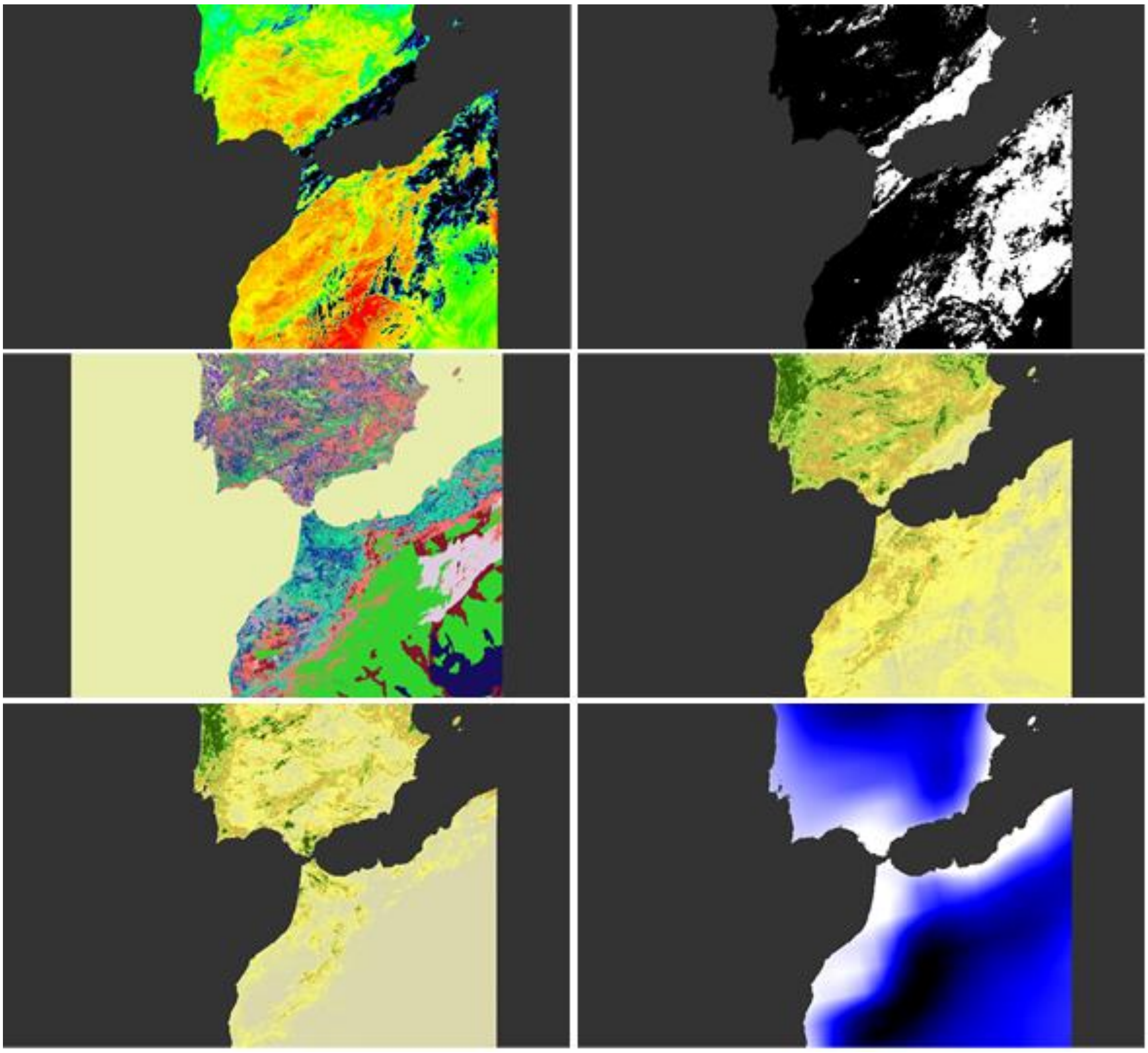

Figure 10: Example data for a PDU of the SL_2_LST product: LST (top left); cloud mask (top-right); biome (middle-left); NDVI (middle-right); fractional vegetation cover (bottom-left); water vapour (bottom-right).

6.2.2 Fire Radiative Power

The SL_2_FRP product is generated from the input Level-1 3-minute PDUs (granules). Each Level-2 FRP product granule consists of an XML manifest (xfdumanifest.xml) and a set of sixteen to eighteen measurement and annotation data files in NetCDF-4 format (depending on the selected SWIR band). Information related to the AF detections and their FRP is stored as two different datasets, both of which are loaded when SNAP is used to open the FRP xfdumanifest.xml manifest file. These datasets are provided in 3 different files, each of them corresponding to a SLSTR image grid. All fires detected using Thermal radiometrical measurements are provided into FRP_in.nc file. SWIR radiometry is also used to detect fires but only during nightime. Results are provided into FRP_an.nc and/or FRP_bn.nc files depending on the selected SWIR band.

Primarily because the number of AF pixel detections is expected to be many orders of magnitude smaller than the total number of image pixels, the first dataset provided - in each measurement file - is a 'LIST' of the characteristics of each confirmed active fire pixel. FRP_in.nc, FRP_an.nc and FRP_bn.nc NetCDF files contain no information from non-fire pixels, so are typically quite short. Data stored here include the FRP estimate for each confirmed AF pixel, together with its FRP uncertainty, AF detection confidence, the time and position of the measurement, and various other auxiliary data. The full list of parameters held as 1D arrays within the List dataset can be found in Table 7, and appears under the folder Metadata when the FRP product xfdumanifest.xml manifest file is opened in SNAP (Figure 11).

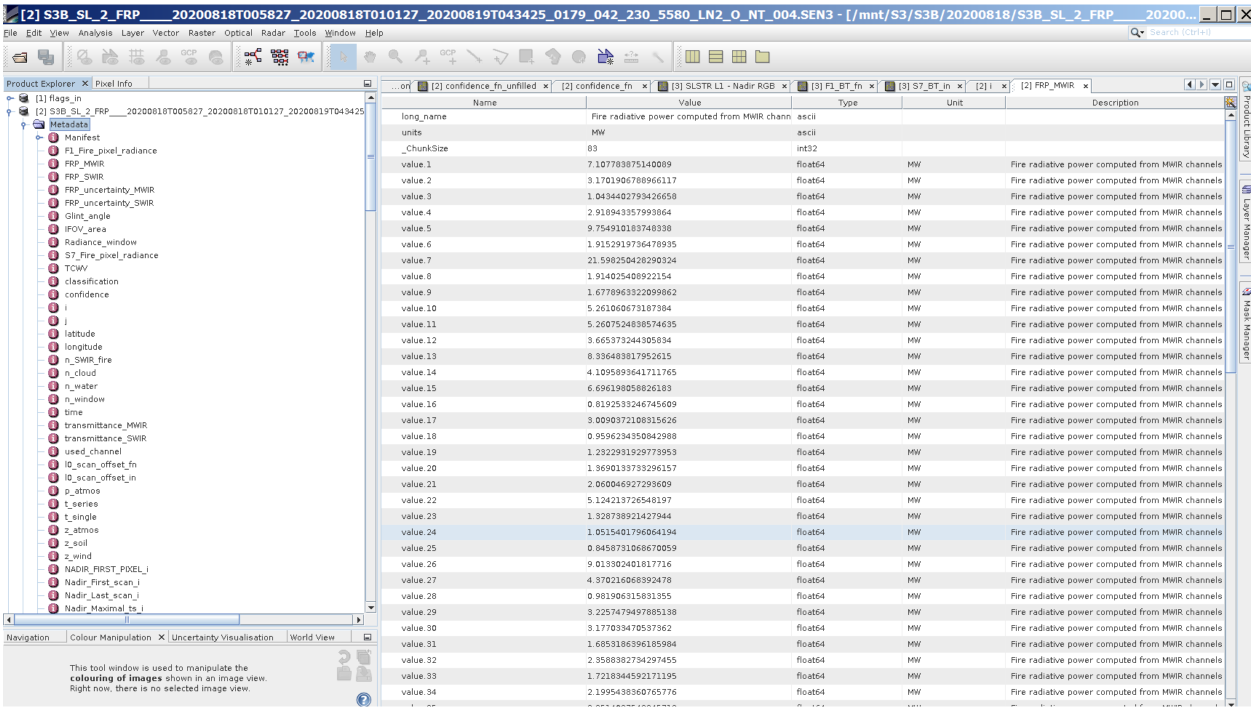

Figure 11: Parameters held within the List dataset of the Level-2 FRP Product file, as displayed in SNAP.

Inside FRP_in.nc file, parameter **FRP_MWIR** stores the FRP in MW of the detected AF pixel, **FRP_uncertainty_MWIR** stores the uncertainty in MW, and **i**, **j** stores the pixel across- and along-track index, whilst its geographic coordinates are stored in **latitude**, **longitude**. Figure 121 shows the List dataset related to the FRP retrievals at the detected active fire pixels (**FRP_MWIR**) openend and displayed in Panoply.

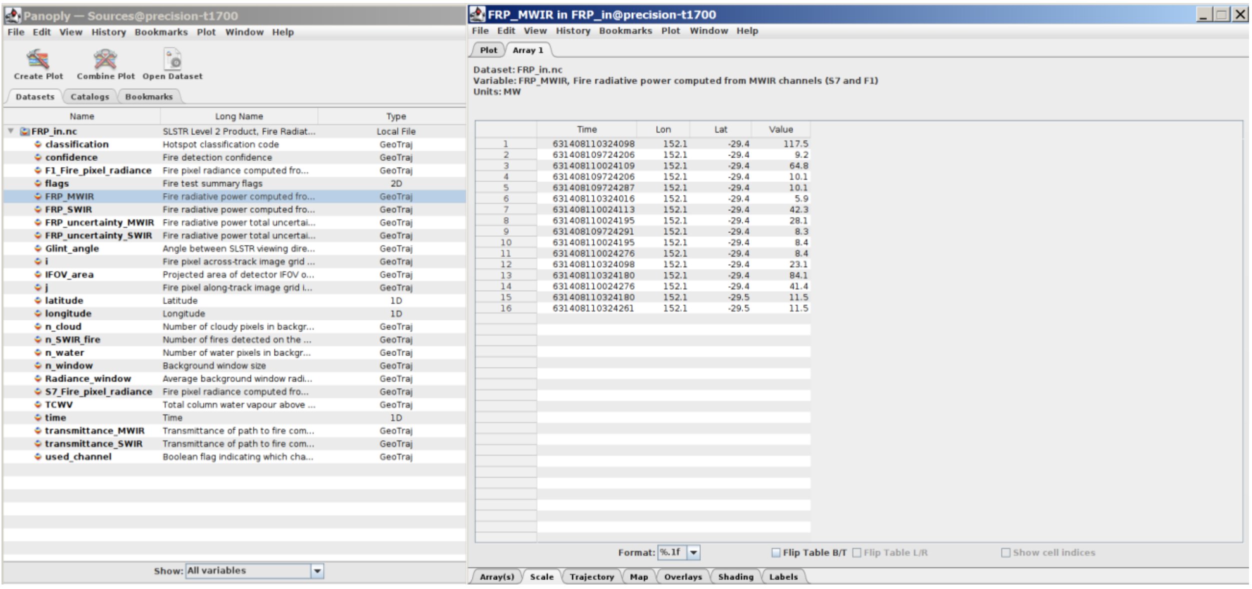

Figure 12: Parameters held within the List dataset of the Level-2 FRP Product file, as displayed in Panoply.

Table 7: Information that is held within the List component of the Level-2 SLSTR FRP_in.nc product file.

Name	Units	Comment
i		Active Fire pixel across-track image grid index
j		Active Fire pixel along-track image grid index
time	µs	Time in microseconds since 1 Jan. 2000
latitude	degrees	Latitude
longitude	degrees	Longitude
FRP_MWIR	MW	Fire radiative power computed from MWIR channels (S7 and F1)
FRP_uncertainty_MWIR	MW	Fire radiative power total uncertainty computed from MWIR channels (S7 and F1)
transmittance_MWIR		Transmittance of path to fire computed from MWIR channels (S7 and F1)
classification	See Table 8	Hotspot classification code
S7_Fire_pixel_radiance	$W/m^2/sr/\mu m$	Fire pixel radiance computed from S7 brightness Temperature
F1_Fire_pixel_radiance	$W/m^2/sr/\mu m$	Fire pixel radiance computed from F1 brightness Temperature
used_channel		Boolean flag indicating which channel was used in the FRP calculation, with 0 referring to S7 channel and 1 to F1 channel
Radiance_window	$W/m^2/sr/\mu m$	Average background window radiance used in the FRP equation. This radiance is associated with the channel defined by the used_channel parameter
Glint_angle	degrees	Angle between nadir view and specular direction

Name	Units	Comment
BT_MIR	Kelvin	MIR Brightness Temperature from the fire
BT_window	Kelvin	Mean Brightness Temperature of the valid pixels in the background window
Sun_zenith_angle	Degrees	Solar Zenith angle
Satellite_zenith_angle	degress	Satellie View Zenith angle
Day/night		Daytime or nighttime fire flag set to 1 in case of daytime (i.e. Solar zenith angle < 85 degree.)
IFOV_area	m^2	Projected area of detector IFOV on surface
TCWV	kg/m^2	Total column water vapour above fire
n_window		Background window size
n_water		Number of water pixels in background window
n_cloud		Number of cloudy pixels in background window
flags	See Table 10	Fire test summary flags

Table 8: FRP classification byte values for the List product parameter 'Classification'.

Bit number	Text code	Description
0	*vegetation_fire*	*If raised, suspected vegetation fire*
1	*onshore_gas_flare*	*if raised, suspected onshore gas flare*
2	*offshore_gas_flare*	*if raised, Suspected offshore gas flare*
3	*volcanic*	*if raised, Suspected volcanic hotspot*
4	*industrial*	*if raised, Suspected industrial hotspot*

FRP_an.nc and FRP_bn.nc includes similar parameters than FRP_in.nc with the addition of :

- Fire Radiative Power computed from SWIR channels and the associated uncertainties and transmittance.
- A ratio of the radiances measured in S5 and S6 indicating whether the AF pixel detection is likely to be from a vegetation fire or a gas flare (Values sup. or equal to to 0.9)
- All radiometric elements such as Radiance_window or Fire_pixel radiance are associated with SLSTR S5 and S6 channels instead of S7 and F1 channel

Table 9: Information that is held within the List component of the Level-2 SLSTR FRP_an.nc/bn.nc product file.

Name	Units	Comment
i		Active Fire pixel across-track image grid index
j		Active Fire pixel along-track image grid index
time	µs	Time in microseconds since 1 Jan. 2000
latitude	degrees	Latitude
longitude	degrees	Longitude
FRP_MWIR	MW	Fire radiative power computed from MWIR channels (S7 and F1)
FRP_SWIR	MW	Fire radiative power computed from MWIR channels (S6 channel)
FRP_uncertainty_SWIR	MW	Fire radiative power total uncertainty computed from SWIR channels (S6) and associated with the detected SWIR fire
transmittance_SWIR		Transmittance of path to fire computed from MWIR channels (S6 channel)
Ratio_S56		Ratio of the radiances measured in S5 and S6 indicating whether the AF pixel detection is likely to be from a vegetation fire or a gas flare (Values sup. or equal to to 0.9)
S5_confirm		This flag indicates if this fire has been detected using both S6 and S5 radiances (equal to 1) or only using S6 (value = 0)
classification	See Table 8	Hotspot classification code
S6_Fire_pixel_radiance	W/m^2/sr/µm	S6 Fire pixel radiance
F5_Fire_pixel_radiance	W/m^2/sr/µm	S5 Fire pixel radiance
used_channel		Boolean flag indicating which channel was used in the FRP calculation, with 0 referring to S7 channel and 1 to F1 channel
Radiance_window_S6	W/m^2/sr/µm	Average S6 background window radiance used in the FRP equation.
IFOV_area	m^2	Projected area of detector IFOV on surface
TCWV	kg/m^2	Total column water vapour above fire
flags	See Table 11	Fire test summary flags

The second category of dataset held within the Level-2 FRP product file is generated on the image grid, and consists of a 2D 'SUMMARY FLAG' dataset providing the results of the various active fire detection tests and associated processing steps from the List dataset for every pixel in the Level-1 granule, whether or not it was detected as an AF pixel. This Summary Flag dataset is consequently far larger than the list dataset. The Summary Flag dataset is stored as FLAGS in the **FRP_in.nc** NetCDF file (see Table 7) and in the FRP_an.nc and FRP_bn.nc (see Table 11). Figure 13 shows an example of Summary Flag data opened in SNAP, in this case the 'high confidence fire' flag. In SNAP the 'Pixel Info' window can be used to examine which of the various flags shown in Table 10 are set for each pixel in the granule.

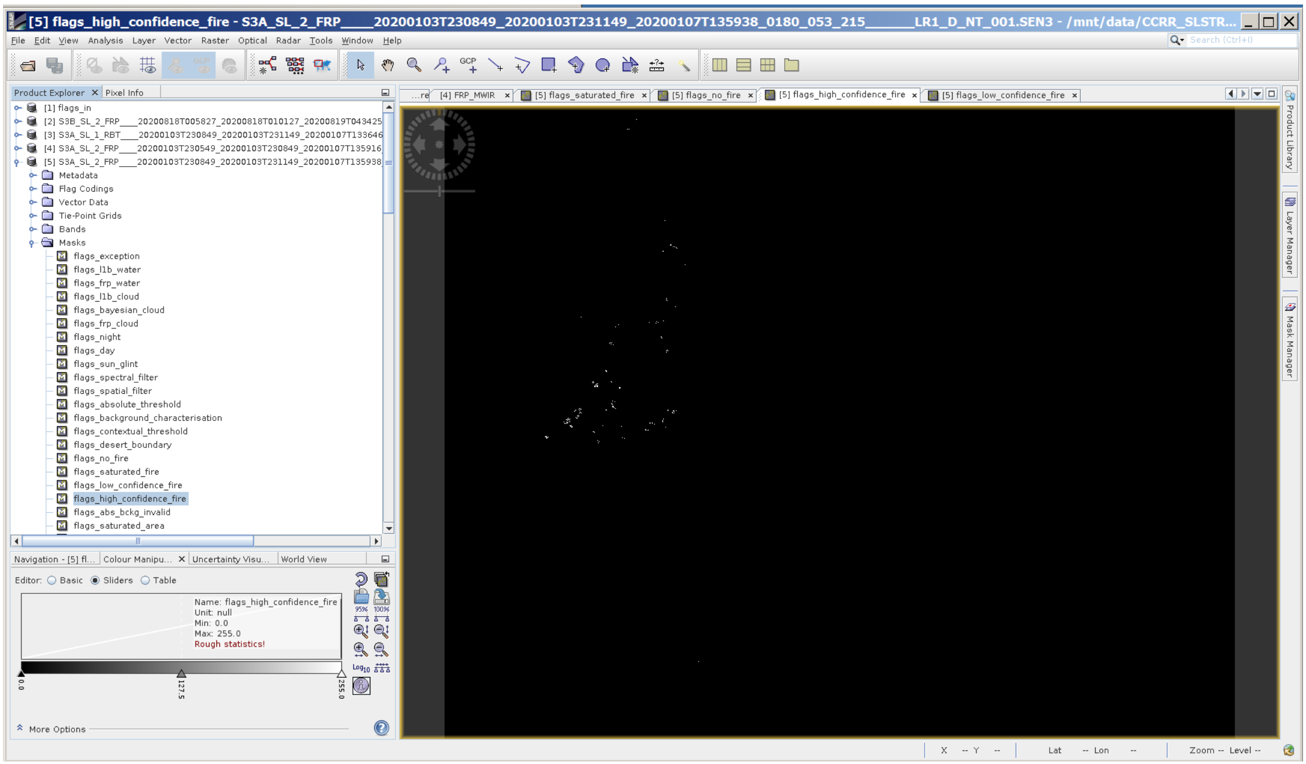

Figure 13: Parameters held within the Summary Flag dataset of the Level-2 FRP Product file, as opened in SNAP. The 'high confidence fire' mask of detected active fire pixels is shown displayed and full set of parameters is provided in Table 10.

Table 10: FRP Summary Flag byte values held in the List component of the Level-2 FRP_in.nc product file.

Bit number	Value	Text code	Description
0	1	*exception*	*L1b pixel radiance exception*
1	1	*l1b_water*	*L1b water surface classification*
2	1	*frp_water*	*Water detected by FRP tests*
3	1	*l1b_cloud*	*Cloud detected by L1b tests*
4	1	*bayesian_cloud*	*Cloud detected by Bayesian tests*
5	1	*frp_cloud*	*Cloud detected by FRP tests*
6	0	*night*	*Pixel is in day or night*
	1	*day*	
7	1	*sun_glint*	*Sun glint*
8	1	*spectral_filter*	*Potential fire identified by spectral test*
9	1	*spatial_filter*	*Potential fire identified by spatial test*
10	1	*absolute_threshold*	*Fire identified by absolute threshold test*
11	1	*background_characterisation*	*Potential fire successful background characterisation*

Bit number	Value	Text code	Description
12	1	*contextual_threshold*	*Potential fire confirmed by contextual threshold test*
13	1	*desert_boundary*	*Potential fire rejected by desert boundary test*
14	0	*Normal F1 BT*	*Pixels have F1 BT < saturation BT according to L1b quality flag*
	1	*Saturated F1 BT*	*Pixels have F1 BT > saturation BT according to L1b quality flag*
15	0	*Pixels that are not fire pixels*	*Normal pixels*
	1	*Fire pixels*	*Confirmed Fire pixels*
16	1	*abs_bckg_invalid*	*If raised, Fire detected by absolute test but associated with unvalid background*
17	1	*saturated_area*	***If raised, pixel in located on a saturated area (i.e the percentage of S7-saturated pixel are higher than a certain threshold) and "classic" FRP detection cannot be processed over this pixel***
18	1	*cloud_edge*	*If raised, this potential fire pixel has been discarded due to neighboring cloudy pixels*
19	1	*land-water_edge*	*If raised, this potential fire pixel has been discarded due to too many neighbors with inconsistent surface classification.*
20	1	*F1_downscan*	*If raised, this pixel has been discarded from processing due to a possible F1 downscan anomaly*

Table 11: FRP Summary Flag byte values held in the List component of the Level-2 FRP_an/bn.nc product file.

Bit number	Value	Text code	Description
0	1	*exception*	*L1b pixel radiance exception*
1	1	*l1b_water*	*L1b water surface classification, derived from 1 km grid*
2	1	*frp_water*	*Water detected by FRP tests, derived from 1 km grid*
3	1	*l1b_cloud*	*Cloud detected by L1b tests, derived from 1 km grid*
4	1	*bayesian_cloud*	*Cloud detected by Bayesian tests, derived from 1 km grid*
5	1	*frp_cloud*	*Cloud detected by FRP tests, derived from 1 km grid*
6	0	*night*	*Pixel is in day or night, derived from 1 km grid*
	1	*day*	
7	0	*Pixels that are not fire pixels*	*Normal pixels*
	1	*Fire pixels*	*Confirmed Fire pixels*
8	1	*S6_absolute*	*Fire Pixel successfully detected by S6 absolute test*
9	1	*S5_absolute*	*Pixel successfully detected by S5 absolute test*

6.3 Level-1 product content

The Level-1 product consists of 97 separate NetCDF files, along with a manifest file. The full product is very large (~400MB), and unless you want to view its entire contents in SNAP (see Section 8.1.2), it may not be necessary to download every individual NetCDF file. The data structure allows for files to be downloaded separately or in specific groups. The different 'families' of files are described below.

6.3.1 Channel pairs

Each channel has a pair of files giving the radiance/brightness temperature and associated quality information. Each channel pair is available for the two SLSTR views (nadir and oblique).

- **S*_radiance, S*_BT:** Channels S1-S6 report the observed scene in ***radiance*** and S7-S9, F1-F2 report the observed scene in ***brightness temperature*** (*BT)*. If any pixel contains bad data, it will contain a standard '_FillValue' (e.g. NaN) and the reason will be provided in the 'exception' code. The exception code could also be raised if good data are found in the pixel (e.g. in the case of cosmetically filled pixels). The radiances or BTs of the orphan pixels are included in this file too.
- **S*_quality:** Each channel also has a *quality* file associated with it providing channel-specific information such as measurement uncertainties, instrument specific information, detector gains, temperatures, etc. A particularly useful quantity in the *radiance quality* files are the solar irradiance values that can be used to transform the radiance to reflectance (see Section 8.2.9).

6.3.2 Channel-grid families

The location of each pixel on the Earth, its altitude, cloud cover, type of surface being viewed, as well as more detailed information that allows the pixel to be traced back to its origin in the instrument frame of reference, are provided in image grid files, shared between 'channel pairs' of the same *grid*.

The images are provided on 4 different types of grid. Radiances measured by channels S1-S6 are provided on a 0.5 km spatial resolution grid referred to as the '**a-grid**'. Radiances measured by channels S4-S6 are also provided on a second grid, the '**b-grid**' at 0.5 km spatial resolution. The b-grid is specific to S4-S6 and arises due to the fact that the SWIR channels use a detector array of 4×2 elements, an 'a-stripe' and a 'b-stripe', rather than a single 4×1 element stripe as used by the visible channels. The a-stripe of the SWIR channels is optically aligned to the 1×4 VIS detector elements, hence each is referred to as the '**a-grid**'. The b-stripe of the SWIR channels is processed separately and is mapped to its own grid, as the b-stripe detectors view a physically different point on the ground. There are two detector stripes for the SWIR channels because they were originally intended to allow for a time domain integration of these stripes to improve the signal-to-noise ratio, but are now provided separately for users.

Brightness temperatures measured by channel S7-S9 and F2 are provided on a 1 km spatial resolution grid referred to as the '**i-grid**'. It is this grid that the LST and FRP product are mapped to. Brightness temperatures measured by channel F1 are provided on a 1 km spatial resolution grid referred to as the '**f-grid**'. This channel has its own grid because its detectors are offset slightly from the other infrared channels.

The data provided on these grid-specific files and shared between channels of the same grid are as follows:

- **geodetic**: Contains the measurement pixel latitude, longitude and surface elevation. The coordinates are 'ortho-rectified', meaning that the elevation of the Earth's surface has been taken into account.
- **flags**: Contains auxiliary information for each pixel such as the surface type (ocean, land, tidal, coast, inland water), illumination (day, twilight, sunglint), status of gridding (cosmetic, duplicate), cloud mask (combined and individual cloud test results, Bayesian – see Section 8.2.15), pointing flags (indication of problems in scanning). More detailed information on this file is provided in the *L1 PDFS*.
- **cartesian**: Contains the quasi-Cartesian (x, y) coordinates of each pixel. The origin of this coordinate system is the sub-satellite point (x=0) and the pixel closest to the ANX, where the satellite crosses the equator moving from South to North (y=0). It should be noted that the y=0 coordinate of a product may refer back to the ANX of the previous orbit, rather than the current one.
- **indices**: It is important that each image pixel can be traced back to its original measurement by the instrument. This file provides the instrument level scan, pixel and detector origins and would only be used for very specific purposes (e.g. see Section 8.2.6).
- **time**: Contains the information needed to reconstruct the acquisition time of each measurement - see Section 8.2.6.

There is additional information that is provided on a 5^{th} grid referred to as the '**tie-point grid'**. This grid has a spacing of 16 km in the across track direction and is used for parameters that do not need to be provided at full resolution. See Section 8.2.5 for details of how to interpolate the tie point parameters to the image grid.

- **geometry**: One file is provided for the nadir view, and one for the oblique view. This contains the viewing and solar angles.
- **met**: The meteorological data file is shared by both views. It contains information taken from meteorological models on the state of the atmosphere and other useful meteorological data. Note that these are not direct measurements, but ancillary data provided near to the times and locations of the SLSTR images, derived from the European Centre for Medium-Range Weather Forecasts (ECMWF).

7 Data Quality Information

7.1 Radiometric quality

Uncertainties in the radiometric calibration are provided in the Level-1 quality annotation datasets. For each spectral band uncertainties are reported for:

- Random effects - detector noise expressed as NEDT (TIR channels) and NEDL (VIS/SWIR channels) for each scan line
- Correlated effects - radiometric calibration are included in the quality annotation datasets as a table of uncertainty vs. temperature type-B (a-priori) estimates based on the pre-launch calibration and calibration model.

Currently, per pixel estimation of the radiometric uncertainty for either random or correlated (systematic) effects has not been implemented. However it is possible to map the uncertainty information from the quality dataset to the image. This process is explained in the FAQ section 8.2.

7.1.1 Thermal Infrared Channels

Verification of the thermal infrared channel calibration was performed during extensive pre-launch calibration campaigns. Tests were performed under thermal-vacuum conditions with the instrument in full flight configuration to validate the on-board calibration systems, and the processing algorithms and auxiliary data used in the operational data processing system to convert from raw data to calibrated radiances and brightness temperature. Results from the instrument-level calibration tests provide key inputs into the Level-1 data processing chain, in-particular the non-linearity tables and stray light correction factors. For a more detailed description of the test activities and results it is recommended to refer to Smith et al. (2020).

In summary, the BTs measured by both SLSTRs agreed within the 0.1 K goal, after correcting for non-linearity and stray light effects, over the range 240 K to 320 K, and the radiometric noise performance exceeded the requirements and was within the predicted budget.

Table 12: SLSTR-A and B uncertainties expressed as BT in mK from pre-launch tests for SLSTR IR Calibration for a reference scene temperature at 270 K (Smith et al., 2020).

	SLSTR-A			SLSTR-B		
	S7	S8	S9	S7	S8	S9
NEDT (Random)	46	13	20	33	14	17
Combined uncertainty (k = 1)	22	18	18	22	18	18

Analysis of the Sentinel-3 tandem phase comparisons of SLSTR-A and B Level-1 radiometric data reported in Hunt et al. (2020) has confirmed that the relative calibrations of SLSTR-A and B are consistent with the calibration results reported.

7.1.2 Visible/Short Wave Infrared Channels

The calibration factors used in the Level-1 processing were derived from the pre-launch calibration tests at instrument level. Analyses of SLSTR top-of-atmosphere radiances over stable reference sites have been performed by different groups including:

- RAL Space for the MPC comparisons with AATSR and MODIS-A over desert sites.
- CNES assessment using the SADE/MUSCLE vicarious calibration system.
- Radiative Transfer Modelling of the Libya-4 desert site by Rayference.
- University of Arizona comparisons against in-situ field measurements of the Railroad Valley Playa RadCalNet site.

The analyses of the different groups showed good agreement within their reported uncertainties, see Figure 14. Uncertainties in the calibration factors are based on those reported by the different teams and are the best estimates at the time of writing.

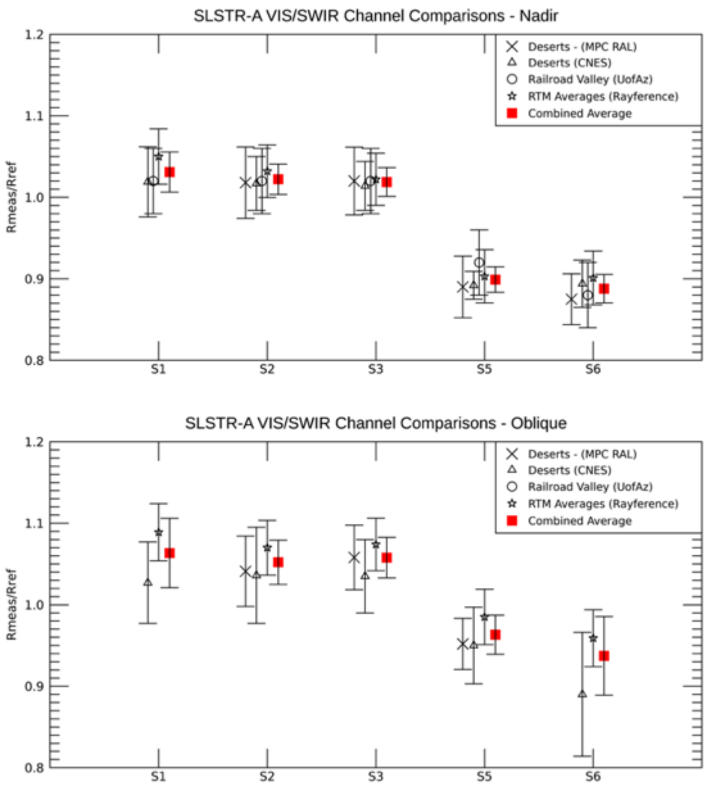

Figure 14: Summary of comparisons of SLSTR VIS/SWIR channel reflectances vs. Reference methods.

The analysis suggests that for the nadir view S1-S3 shows ~3% error relative to the reference sensor (MERIS) and ~5% for the oblique view, while the SWIR channels show ~12% error relative to the reference sensors (MODIS/AATSR) in the nadir view and ~5% in the oblique view. The root cause of this discrepancy is subject to a detailed investigation.

To account for the offsets reported for the current Level-1 products it is recommended that users apply the correction factors provided in Smith (2020), which are provided in Table 13.

Table 13. Recommended correction factors for the VIS and SWIR channels, together with uncertainty estimates. The source of the inputs used for this analysis are also provided. Note that no values are provided for channel S4 as the vicarious calibration methods do not extend to this channel.

Nadir View

	S1	S2	S3	S5	S6
Correction	0.97	0.98	0.98	1.11	1.13
Uncertainty	0.03	0.02	0.02	0.02	0.02
Input Analysis	UoAz Rayference CNES	UoAz MPC (RAL) Rayference CNES	UoAz MPC (RAL) Rayference CNES	UoAz MPC (RAL) Rayference CNES	UoAz MPC (RAL) Rayference CNES

Oblique View

	S1	S2	S3	S5	S6
Correction	0.94	0.95	0.95	1.04	1.07
Uncertainty	0.05	0.03	0.03	0.03	0.05
Input Analysis	Rayference CNES	MPC (RAL) Rayference CNES	MPC (RAL) Rayference CNES	MPC (RAL) Rayference CNES	Rayference CNES

Note: Uncertainty estimates are at k=1.

7.2 Geolocation accuracy

The geometric accuracy of SLSTR-A and SLSTR-B is validated using visible data from channel S3 correlated with ground control points. This shows an accuracy within 0.1 visible pixels (50 m) in nadir view along- and across-track and in oblique view across-track, and slightly larger in oblique view along-track, within 0.2 visible pixels (100 m).

A sub-pixel mis-registration of S7 with regard to S8 and S9 of ~250 m for SLSTR-A and ~120 m for SLSTR-B has been detected and is being investigated.

There is also a mis-registration between the fire channel, F1, and channel S7. This has been partly corrected in the nadir view by the inclusion of a separate F1 coordinate grid (see Section 6.3.2), and the offset is less than 1 km at the centre of the swath, but increases with increasing satellite zenith angle. The offset is larger in the oblique view.

The projected footprint of SLSTR detectors on the ground changes across the swath due to the changing satellite view geometry. The footprint is close to the ideal case at the sub-satellite point, but towards the edges of the swath it is stretched, increasing the area covered (by up to a factor of 6 for channel S7). The effect of this change is significant for sharp features such as fires and coastlines.

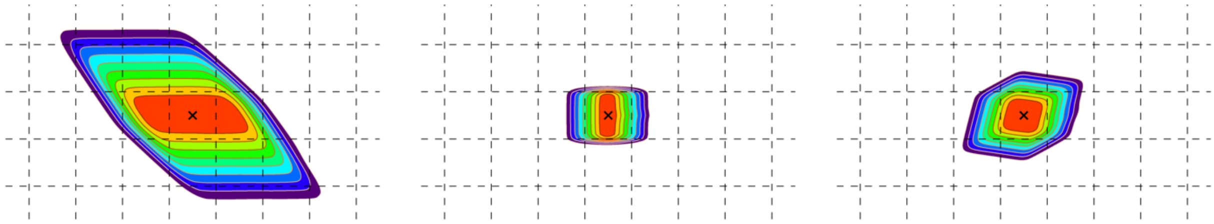

Figure 15: SLSTR-A footprint for channel S7 at the left hand edge, middle, and right hand edge of the nadir swath.

7.3 LST Quality and Validation

The Sentinel-3 LST product is routinely validated in an operational capacity. The validation comprises assessment against in-situ observations (Category-A validation) from twelve ‘Gold Standard’ Stations, and intercomparison (Category-C validation) with respect to an independent operational reference product (SEVIRI from LSA SAF). Higher level products are also evaluated for identifying any gross problems.

Category-A validation uses a comparison of satellite-retrieved LST with in-situ measurements collected from radiometers sited at a number of stations spread across the Earth, for which the highest-quality validation can be achieved. Here we concentrate on twelve ‘Gold Standard’ stations which are installed with well-calibrated instrumentation: seven from the SURFRAD network (Bondville, Illinois; Desert Rock, Nevada; Fort Peck, Montana; Goodwin Creek, Mississippi; Penn State University, Pennsylvania; Sioux Fall, South Dakota; Table Mountain, Colorado); two from the ARM network (Southern Great Plains, Oklahoma; Barrow, Alaska); and three from the USCRN network (Williams, Arizona; Des Moines, Iowa; Manhatten, Kansas).

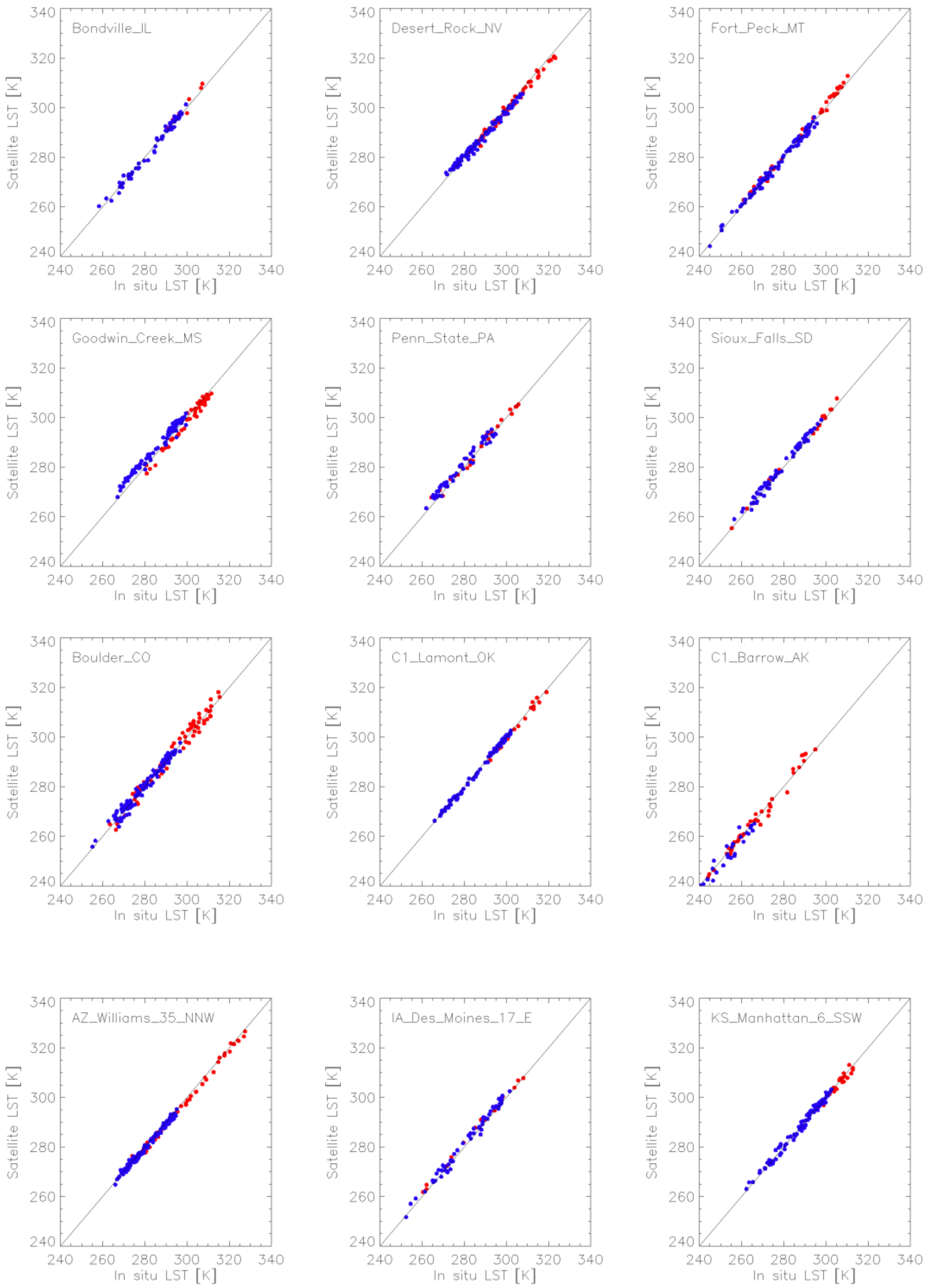

Figure 16: Validation of the Sentinel-3A SL_2_LST product for 2019 at the Gold Standard in-situ stations for the period 1st March 2019 to 31st January 2020.

The accuracy can be directly compared with the mission requirement of 1 K. For both S3A and S3B, overall the absolute daytime and night-time accuracy are within the mission requirements for LST.

Category-C validation uses inter-comparisons with similar LST products from other sources such as other satellite sensors, which give important quality information with respect to spatial patterns in LST deviations. Here we compare the SL_2_LST product from both SLSTR-A and SLSTR-B with the operational SEVIRI L2 product available from the LSA SAF.

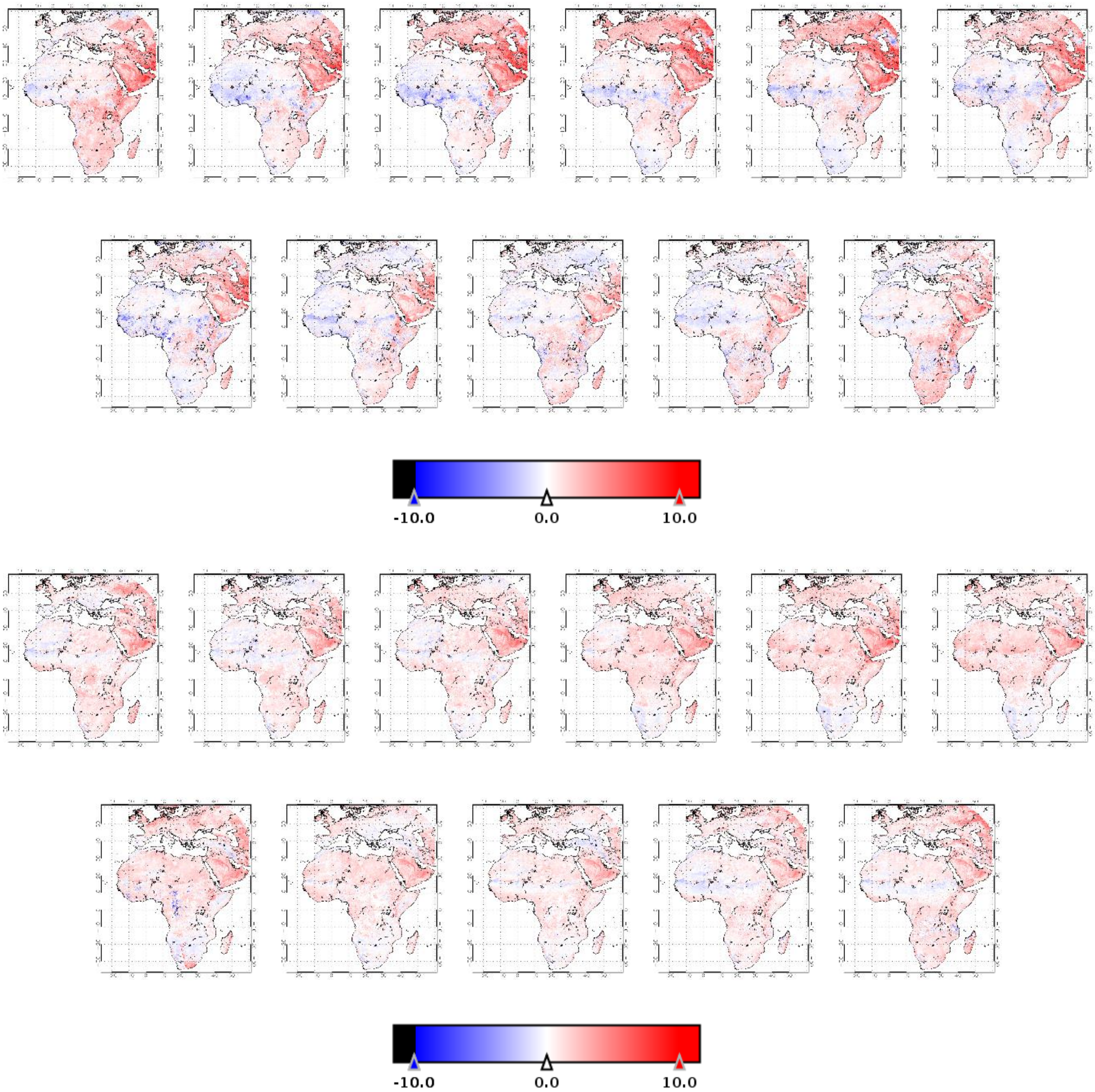

Figure 17: Intercomparison of the Sentinel-3A SL_2_LST product against LSA SAF SEVIRI for each month from March 2019 to January 2020; daytime (top panels); night-time (bottom panels).

The differences are relatively consistent across different land cover types and regions of Europe and Africa. Higher differences occur only in areas of high topographical variance and towards the edge of the SEVIRI disk, a result of the differences in viewing geometry between the two instruments. Comparisons are generally within 1 K and all within the uncertainty range when considering the uncertainties from the reference products, and thus can be interpreted as consistent with each other.

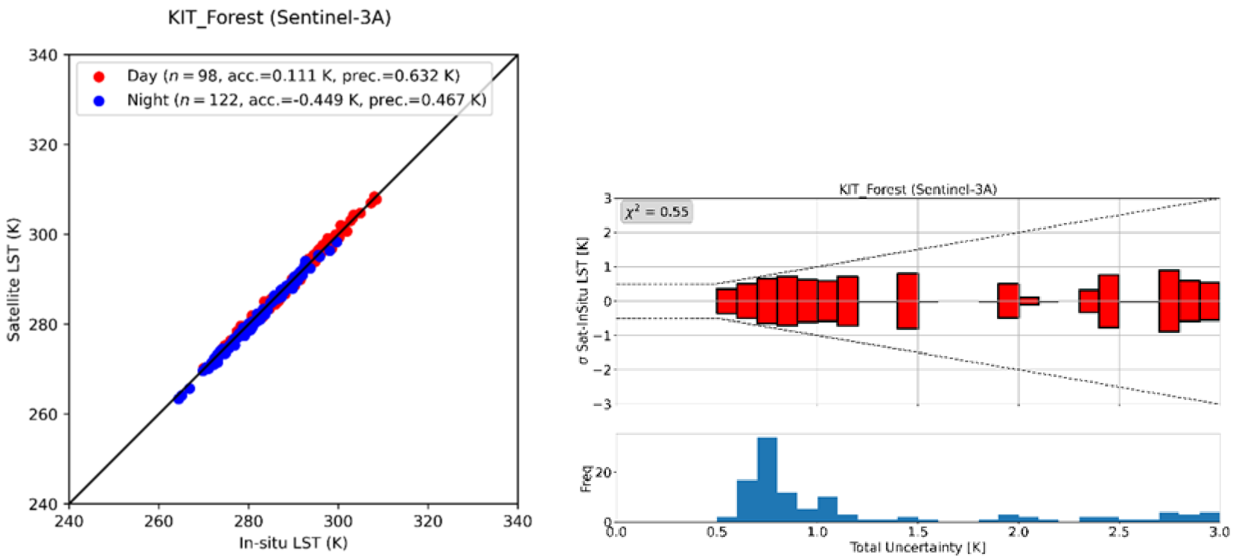

Figure 18: Validation of the Sentinel-3A SL_2_LST product at the KIT Forest in-situ station for the period August 2020 to April 2022 (left); and validation of the associated uncertainties at this site (right).

To ensure quality and credibility of the LST uncertainties, validation of the uncertainties is carried out at select in situ sites where a solid characterisation of the station is available (Figure 18). Of importance is ensuring the LST uncertainty model provides a good representation of the different error effects in the retrieval. For the peak of the matchups between in situ and satellite the LST uncertainties correlate well with the standard deviation of the matchup suugesting a good fit of the uncertainties.

7.4 FRP Quality and Validation

The Sentinel-3 FRP product is subject to continuing quality checks and evaluation, including dedicated validation activities. These have already highlighted issues such as, for example, areas of the ocean where very strong sunglints have saturated some of the VIR channels and thus prevented the sunglint test from operating, which then caused false alarms to appear in the AF detection procedure. Such issues are being tracked and corrected and users are encouraged to identify them to the Helpdesk (Section 8.3) if and when they discover them.

The AF detection process is inherently a trade-off between attempting to detect the lowest FRP fires (which are typically the most common type in most areas), whilst also minimising false alarms. Raising the minimum FRP detection limit in the contextual AF detection algorithm very likely reduces the number of false alarms, but will also prevent some lower FRP fires being identified. Comparison to global data from MODIS Terra taken within a scan angle limit of 30° and within ±6 minutes of a Sentinel-3 acquisition (Xu et al., 2020) shows that 90% of MODIS-identified active fire pixels (MOD14 Collection 6 product) had a matching Sentinel-3 AF pixel detection, representing an apparent SLSTR product commission error compared to MODIS of 10%. Conversely, of the Sentinel-3 AF pixel detections present the same dataset, only 56% had a matching MODIS AF pixel detection, and 79% of the additional detections made by SLSTR had an FRP of less than 5 MW. The additional SLSTR AF detections are mostly below the minimum MODIS FRP detection limit, but SLSTR has a slightly lower minimum FRP detection limit than MODIS and is able to identify them. Work is ongoing to understand how many of these additional SLSTR AF detections are ‘true’ active fires, but it is expected that the vast majority are.

Figure 17 shows the spatial pattern of night-time FRP derived from Sentinel-3B using the prototype of the FRP algorithm compared to that of Terra MODIS for Jan 2019. The patterns are very similar, indicating a good degree of agreement between these two datasets taken at very similar overpass times. The grid-cell FRP totals are also similar since the additional AF pixels that SLSTR detects in many of the grid cells are dominated by low FRP values.

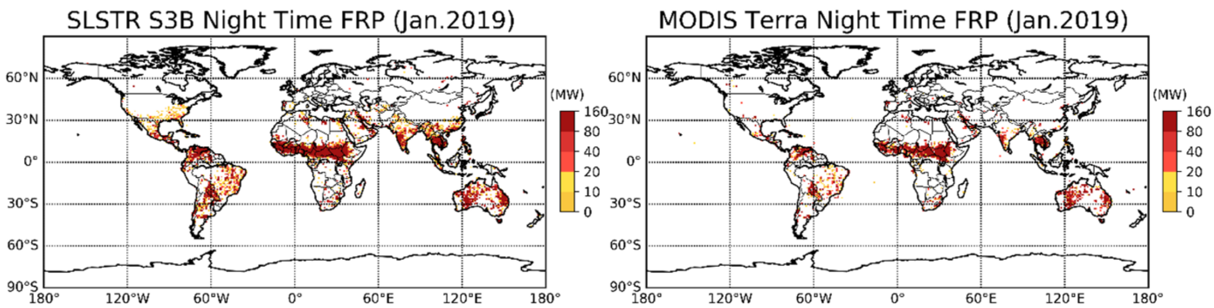

Figure 19: Total FRP of actively burning fires detected within 1° grid cells in January 2019 using Sentinel-3B SLSTR and Terra MODIS data of January 2019.

Figure 18 directly compares the FRP of fire clusters (each comprising a spatially cotiguous set of AF pixels) imaged near simultaneously by SLSTR and by MODIS Terra, and indicates a strong degree of agreement (r^2=0.91), particularly considering that Freeborn et al. (2014) demonstrated a 1 per-pixel MODIS FRP uncertainty of 27%, based only on variability in the sub-pixel location of the fire itself. The slope of the ordinary least squares (OLS) line of best fit exceeds 1.0, primarily because SLSTR quite often detects some low FRP AF pixels at the edge of an active fire cluster that MODIS does not detect (due partly to the smaller ground pixel area of the F1 channel; See Section 5.1.2), and thus the former provides a slightly higher FRP measurement.

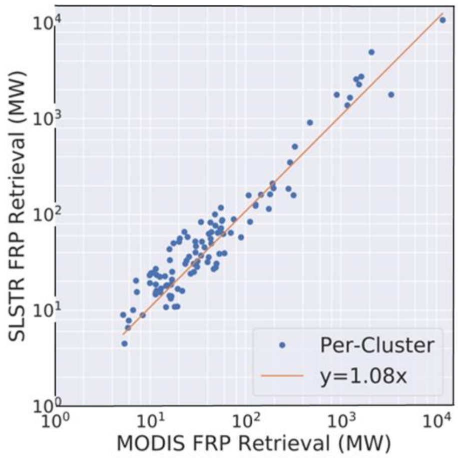

Figure 20: Inter-comparison of night-time global FRP records obtained from Sentinel-3 SLSTR and Terra MODIS within ± 6 minutes of each other. Each measurement is of a single fire cluster, representing a spatially contiguous set of active fire pixels. Both datasets are atmospherically corrected.

Figure 19, shows AF data from three 5° × 5° regions, in terms of both AF pixel count and total FRP for both SLSTR and MODIS throughout January 2019. Temporal patterns are very similar, but SLSTR typically detects more AF pixels than MODIS for the reasons detailed above. However, since these extra AF pixel detections have mostly low FRP values, being located either in smaller AF clusters or at the edges of larger fire clusters, the total FRP assessed by SLSTR each time it images the area is far more similar to that provided by MODIS than is the number of AF pixel detections. Comparisons such as these are ongoing and will ultimately form the basis of transfer functions used to blend the SLSTR and MODIS Terra AF dataset records.

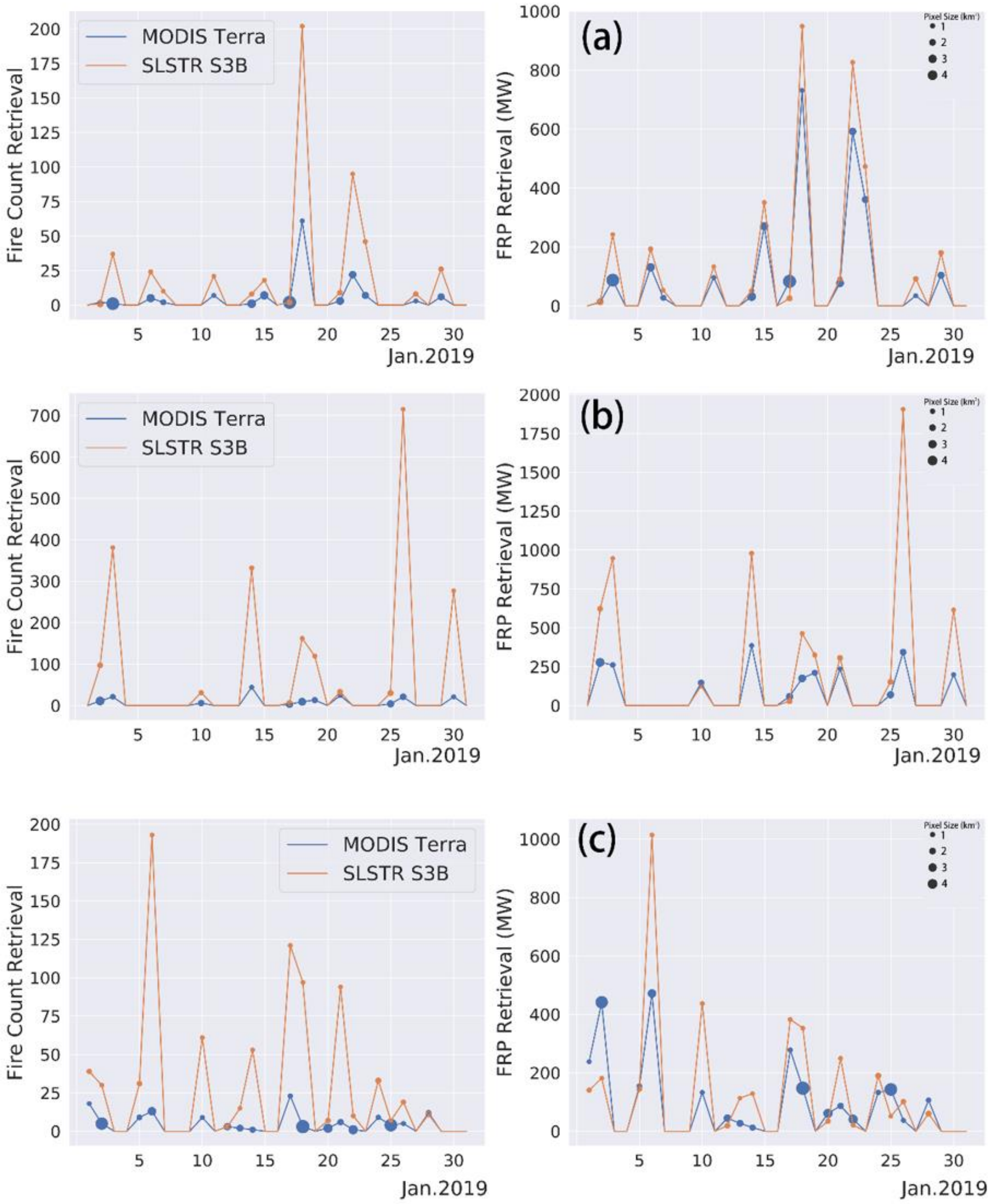

Figure 21: Time Series of total regional AF pixel count (left) and total FRP (right) measured in 5º × 5º geographical areas in (a) South America (Bolivia), (b) West Africa (Guinea), and (c) SE Asia (Vietnam), as derived from Sentinel-3B SLSTR and Terra MODIS in January 2019. Days having no observations are reported as zeros, and the size of the dots represents the pixel area of the instrument's middle infrared channels over the region of interest at that time: F1 (SLSTR) and Band 21 (MODIS). MODIS commonly has a ground pixel area around double that of SLSTR, which helps the latter detect lower FRP fires.

Finally, campaigns where a specially equipped remote sensing aircraft is flown above fires as the Sentinel-3 satellite passes above are starting to provide new and more direct validation data related to the Sentinel-3 FRP product. Figure 20 and Figure 21 show results from such a campaign, conducted in northern Ontario (Canada) where real boreal wildfires were targeted near simultaneously by the aircraft and by the Sentinel-3 satellites. Absolute temporal co-incidence of the aircraft and satellite data is very hard to achieve over dynamic events such as wildfires, so observations were constrained within 30 minutes of one another - noting that the fires FRP would have changed somewhat over even this relatively short timeframe. In the case of the low FRP fire (Figure 22), the degree of agreement between the aircraft and the satellite was within 20%, whereas for the high FRP fire (Figure 21) this was closer to 5%. Typically the FRP uncertainties on low FRP fires are many tens of percent as these fires are close to the minimum detection limit and uncertainties in the estimate of the background radiance can induce significant imprecision, whereas FRP uncertainties on high FRP fires are closer to 10%. This is detailed in Wooster et al. (2015) for example for the Meteosat FRP product, which uses the same FRP uncertainty calculation as deployed in the Sentinel-3 FRP product (see the *FRP ATBD*). Whilst these uncertainties could be considered objectively quite high, it should be remembered that the active fire may cover far less than even 1% of the pixel area, and that the radiance elevation induced by a low FRP fire is of a very similar magnitude to the variation in ambient background spectral radiance seen over the surrounding non-fire pixels. Furthermore, any fire detectable by SLSTR typically shows high variations in its FRP over its lifetime and can even ignite, grow and be extinguished in a matter of hours or even less. As such the FRP measurements provided from low-Earth orbit by SLSTR represent an instantaeous 'snapshot' of this changing phenomena, and rather than specific measurements of individual AF pixels or clusters. The power of these data is thus most strong when providing an overview and an FRP assessment at larger scales of space and/or time rather (e.g. see the Australian fire data shown in Figure 2, or the global-scale maps shown in Figure 19).

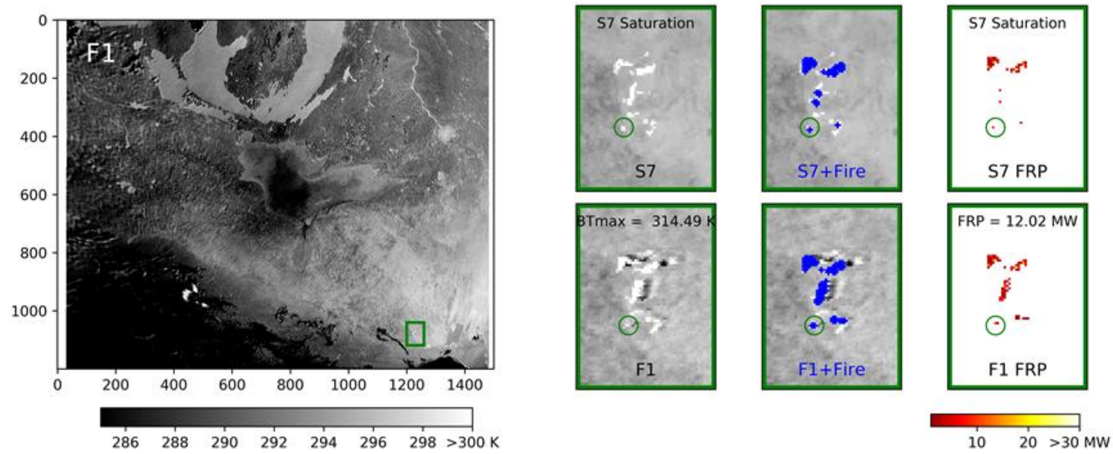

Figure 22: SLSTR data from the S7 and F1 channels over a series of fires in northern Canada in August 2018, some of which were shown previously in Figure 5. Also shown overlain in blue are the locations of the detected AF pixels and circled is the fire whose FRP was near-simultaneously (within 30 minutes) assessed using aircraft remote sensing as 10 MW. This fire was saturated in the S7 channel of SLSTR, but in F1 the FRP was retrieved as 12 MW using data from S3A, and 9 MW using data from S3B (S3A and S3B were operating in tandem mode at this time, and so provided observations closely spaced in time).

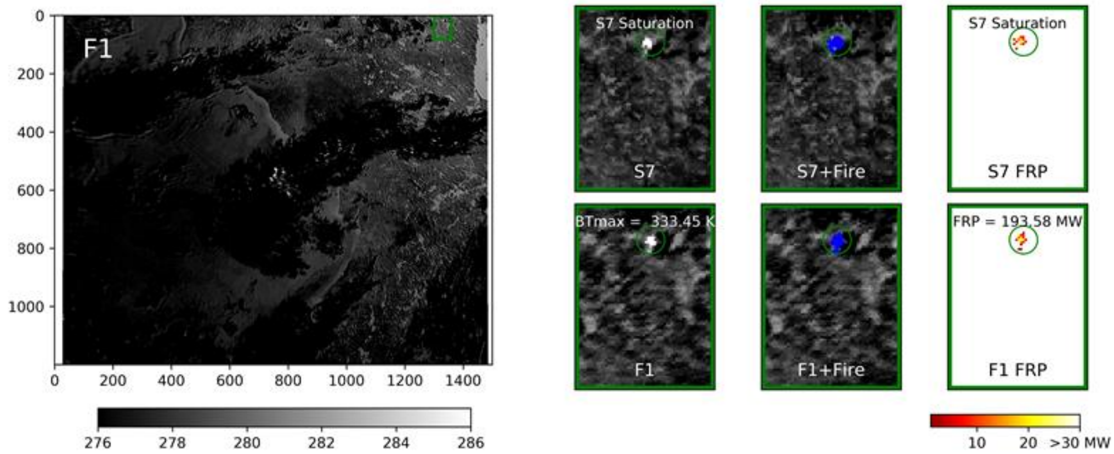

Figure 23: SLSTR data from the S7 and F1 channels over fires burning in northern Canada in a similar area to that shown in Figure 22, but now on a later day in August 2018. Overlain in blue are the locations of the detected AF pixels and circled is the fire whose FRP was near-simultaneously (within 30 minutes) assessed using aircraft remote sensing as 206 MW. This fire was saturated in the S7 channel of SLSTR, but in the S3A F1 channel the FRP was retrieved as 194 MW.

8 Helpdesk

8.1 Access and use of SLSTR products

8.1.1 How to get access to SLSTR products?

The Copernicus programme has adopted a free, full and an open data policy for all users.

The main source of access to SLSTR products is the **Copernicus Open Access Hub**, accessible at: https://scihub.copernicus.eu. A simple self-registration is necessary to access the service. The hub gives also news and further information about the service.

Access can be via a graphical user interface or via the API Hub which allows scripts to be run without going through the graphical interface.

In addition to the download services, Sentinel Data Products are also available in the Copernicus Data and Information Access Service (DIAS) cloud environments. Each DIAS provides processing resources, tools and complimentary data sources at commercial conditions to further facilitate the access to Sentinel data.

8.1.2 How to read and display the SLSTR products?

Since SLSTR products are composed of a set of NetCDF files and a manifest file in xml format, there are many software tools that allow these files to be opened.

In addition to these independent tools (some of which were listed in Section 2), the Sentinel-3 Toolbox is particularly well adapted to SLSTR products. It is composed of a set of visualisation, analysis and processing tools for Sentinel-3 data, based on the Sentinel Applications Platform (SNAP). It is worth noting that it also supports the ESA Envisat (MERIS & AATSR), ERS (ATSR), and SMOS missions as well as third party data from MODIS (Aqua and Terra), Landsat (TM), ALOS (AVNIR & PRISM) and others.

Once SNAP has been downloaded and installed, it is very easy to open SLSTR Level-1 or Level-2 products, by using the xfdumanifest.xml file, from which all other NetCDF files can be read and displayed.

SNAP can be downloaded from http://step.esa.int/main/download/.

8.2 FAQ

8.2.1 Where can I find information about the latest version of processing?

When a new major version of the processing chain is deployed, a Product Notice is released in which the main changes are summarised; the notice gives a status of the performance as well as all known anomalies that are not already fixed. All Product Notices are available on the Sentinel Online web site.

8.2.2 How can I find the version used for the processing of an individual product?

The processing baseline is composed of the processing software (IPF) version and the set of auxiliary data files (ADFs). Any change affecting the version of the IPF or of at least one ADF, increments the version of the processing baseline. Since November 2021, the processing baseline version is indicated in the Product Notice and in the product manifest of all products, along with the individual IPF and ADF versions. Information about successive processing baselines is also available on the Sentinel Online website in the form of a timeline.

The following example shows the IPF software version highlighted in the xfdumanifest.xml file:


```
  <sentinel-safe:processing name="DataProcessing" outputLevel="2" start="2020-11-17T16:09:04.036432" stop="2
    <sentinel-safe:facility name="Land SLSTR and SYN Processing and Archiving Centre [LN2]" organisation="E
      <sentinel-safe:hardware name="OPE"/>
      <sentinel-safe:software name="IPF-SL-2" version="06.16"/>
    </sentinel-safe:facility>
    <sentinel-safe:resource name="S3B_SL_1_RBT____20201117T151706_20201117T152206_20201117T155447_0299_045_
      <sentinel-safe:processing name="DataProcessing" outputLevel="1" start="2020-11-17T15:54:28.189944" s
        <sentinel-safe:facility name="Land SLSTR and SYN Processing and Archiving Centre [LN2]" organisat
          <sentinel-safe:hardware name="OPE"/>
          <sentinel-safe:software name="IPF-SL-1" version="06.17"/>
        </sentinel-safe:facility>
        <sentinel-safe:resource name="S3__AX___CLM_AX_20000101T000000_20991231T235959_20151214T120000___
          <sentinel-safe:processing name="AdfProcessing">
            <sentinel-safe:facility name="ESA Mission Performance Coordinating Centre (MPC)" organisati
              <sentinel-safe:hardware name="OPE"/>
              <sentinel-safe:software name="ADC" version="1.0"/>
            </sentinel-safe:facility>
```


The ADF versions are included separately for each file – for example:


```
</sentinel-safe:resource>
<sentinel-safe:resource name="S3B_SL_1_PCP_AX_20180425T000000_20991231T235959_20190912T120000___________________MPC_O_AL_003.SEN3" r
  <sentinel-safe:processing name="AdfProcessing">
    <sentinel-safe:facility name="ESA Mission Performance Coordinating Centre (MPC)" organisation="ESA Mission Performance Coordin
      <sentinel-safe:hardware name="OPE"/>
      <sentinel-safe:software name="ADC" version="1.0"/>
    </sentinel-safe:facility>
  </sentinel-safe:processing>
</sentinel-safe:resource>
<sentinel-safe:resource name="S3B_SL_1_RTT_AX_20180425T000000_20991231T235959_20180409T120000___________________MPC_O_AL_001.SEN3" r
  <sentinel-safe:processing name="AdfProcessing">
```


8.2.3 How to get information about past anomalies or events?

A specific page is available on the Sentinel Online website providing information about anomalies or events affecting the NTC products:

https://sentinel.esa.int/web/sentinel/technical-guides/sentinel-3-slstr/anomalies-and-events

In addition, monthly Reports are published which detail the instrument performance and anomalies:

https://sentinel.esa.int/web/sentinel/technical-guides/sentinel-3-slstr/data-quality-reports

8.2.4 Why are there sometimes blank areas in the thermal channel images?

The S7 detectors start to saturate at brightness temperatures above 305 K and are saturated around 311 K. For products processed before January 2020, image pixels with a BT above 305 K were filled with NaN and flagged as 'invalid_radiance'. Since January 2020, the pixels above 305 K are still flagged, but are not filled with NaN. These values above 305 K should be treated with extreme caution, and it should be noted that the signal becomes truly saturated around 311 K. In these cases, it is preferable to use the F1 channels instead (as is done in the FRP algorithm).

In a similar way, channels S8 and S9 could also have blank areas for very hot or very cold regions – in these cases, it is because the raw signal is out of the dynamic range of the channel, and will be flagged as saturated (signal above 65535 counts) or no_signal (signal below 0 counts).

8.2.5 How to interpolate from tie point to image grid?

The tie point grid is a more coarsely sampled grid used to store the geometry (Level-1) and meteorological parameters (Level-1 and 2). The grid spacing is 16 km in across- and 1 km in along-track directions. There are three metadata parameters in all product files that allow easy interpolation between tie point and image grids:

Metadata	Definition	Image grid example	Tie point example
RESOLUTION	Size of image pixel in metres in [across-track, along-track]	[1000, 1000]	[16000, 1000]
START_OFFSET	Offset of first image row from ANX of reference orbit in image pixels.	43199	43199
TRACK_OFFSET	Offset of first image column (left side of image) to sub-satellite track in image pixels.	998	64

By reading and comparing these three parameters it is possible to align or interpolate the files on different grids by referencing the pixel index scale, without needing the coordinate files (although the coordinates are also provided on the image and tie point grids for more accurate interpolation – see note on possible misalignment below). For example, the interpolation from tie point to image grid can be achieved by recalculating the image grid pixels as fractions of the tie point pixels. It should be noted that in some products, when interpolating the tie points to the 500m grid, there may be one image row outside of the tie points at the start or end of the product. In this case, the missing tie point row must be retrieved from the adjacent product (or extrapolation used).

One of the key requirements of the tie point grid is that it must be continuous around an orbit. The first tie point is therefore referenced to the ANX. However, this leads to a possible sub-pixel misalignment between tie and image rows in the along-track direction. This misalignment manifests as an arbitrary offset between the image grid and the tie point grid that is found to vary around an orbit.

Finally, note that the files on the tie point grid are symmetrical around the satellite track, whereas the nadir view swath is not symmetrical.

8.2.6 How to calculate the acquisition time of any pixel in a L1/L2 image?

The acquisition time of individual image pixels can be calculated using the 'time' and 'indices' NetCDF files in the Level-1 product. The time of image pixel, *i,j*, in the nadir view can be calculated from:

$$T_{i,j} = T_{init} + (S_{i,j} - S_{init})\Delta t_{scan} + (P_{i,j} + P_{0\text{-}nadir})\Delta t_{pixel}$$

where $S_{i,j}$ and $P_{i,j}$ are the scan and pixel numbers from *indices_in.nc*, and the other variables are from *time_in.nc* as shown below:

Parameter	Var	Definition
NADIR_MINIMAL_TS_I	T_{init}	Timestamp of first scan in the image row (at acquisition pixel zero)
NADIR _FIRST_SCAN_I	S_{init}	Scan number of first scan in the image row
SCANSYNC	Δt_{scan}	Time for one complete scan (one rotation of the scan mirror = 299.985 ms)
NADIR_FIRST_PIXEL_I	$P_{0\text{-}nadir}$	Acquisition pixel number at the start of the nadir swath
PIXSYNC	Δt_{pixel}	Time between acquisition pixels within each scan (81.74 µs)

8.2.7 How to calculate the relative angle between the satellite and Sun?

The solar and satellite elevation and azimuth angles are provided in the Level-1 product on the tie point grid in the *geometry_tn.nc* and *geometry_to.nc* files.

8.2.8 How to convert from brightness temperature to radiance in the Level-1 product?

The Level-1 brightness temperature measurements provided for the thermal channels (S7-S9, F1 and F2) can be converted to radiance by integrating the Planck function at the BT of interest multiplied over the spectral response of each band. The spectral response functions for SLSTR-A and SLSTR-B are available on the ESA Sentinel Online website (see Section 8.2.10)

8.2.9 How to convert from radiance to reflectance in the Level-1 product?

The visible and SWIR channels (S1-S6) provide measurements of top of atmosphere (ToA) radiances (mW/m^2/sr/nm). These values can be converted to normalised reflectance for better comparison or merging of data with different sun angles as follows:

reflectance = π (ToA radiance / solar irradiance /* COS*(solar zenith angle))*

where the solar irradiance at ToA is given in the 'quality' dataset for the channel, and the solar zenith angle is given in the 'geometry' dataset. The solar irradiance contained in the quality dataset is derived from the solar spectrum of Thuillier et al. (2003) integrated over the measured SLSTR spectral responses and corrected for the earth-to-sun distance at the time of the measurement.

8.2.10 How to find the SLSTR spectral response functions?

The SLSTR spectral response functions are provided on the Sentinel Online webpages:

https://sentinel.esa.int/web/sentinel/technical-guides/sentinel-3-slstr/instrument/measured-spectral-response-function-data

8.2.11 How to find the centre of the swath in the image?

The SLSTR oblique swath is symmetrical about the Sentinel-3 satellite track, but the nadir swath is not. The image column closest to the satellite track (i.e. that crosses the sub-satellite point) can be found by using the TRACK_OFFSET metadata item in the product or manifest file (see also Section 8.2.5).

8.2.12 What is cosmetic filling?

The nearest-neighbour re-gridding algorithm leads to some image pixels with no measurement sample. These empty pixels are filled by copying across one of the 8 neighbouring pixels. In the image below, the arrows show which of the surrounding pixels have been used to fill the empty image pixel. The pixel chosen to be copied, is the one which is located closest to the empty image pixel ('orphans' are also considered). The image pixel that has been filled with the copy is now referred to as being **'cosmetically filled'** and is flagged in the dataset. Note that cosmetically filled pixels only appear in the Level-1 data, and are ignored in the Level-2 processing.

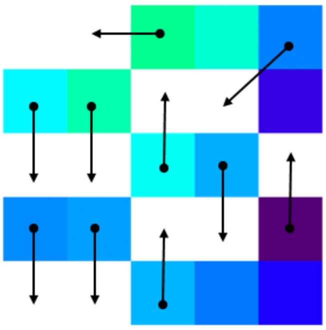

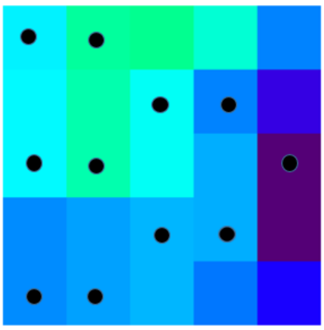

● Cosmetic image pixel

8.2.13 What is an orphan pixel and are they useful?

Sometimes there is more than one candidate measurement pixel that could be used to fill an image pixel in the re-gridding process. When this happens, the measurement that is closest to the centre of the image pixel is used, and all the other instrument pixels that might have been used to fill it are saved as '**orphan pixels**' in the dataset so that they can still be used if desired. The image pixel that has several candidates is flagged as '**duplicate**' to show that there are other measurements that may be of interest.

The following example shows a zoomed-in part of a Level-1 image showing a series of gas flares. These appear as very hot pixels. The left image is the re-gridded L1 image and the centre is the image in the instrument frame. In the process of regridding the instrument pixels, some were made '**orphans**' in the process and were not used in the final Level-1 image - these are shown in white in the right hand plot. Two hot pixels are circled in the centre image, as these are missing from the Level-1 image but are retained in the product as orphans. It may be important to consider the presence of orphans for users interested in small-scale features.

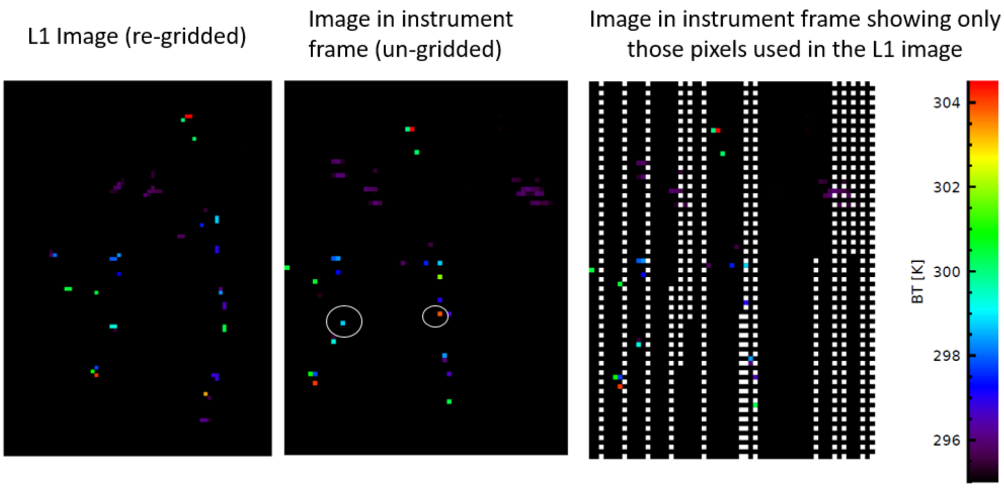

8.2.14 Why is there a stripe of unfilled pixels at the sides of the image?

Sometimes it isn't possible to fill an empty image pixel cosmetically during the Level-1 re-gridding process (see Section 8.2.12) as there are no valid pixels surrounding it. This often happens at the edge of an image. In this case, any image pixels are labelled as '**unfilled**', and the edge of an image can appear jagged depending on exactly how the measurements fall over the image grid. As the image grid is created to be slightly larger than needed, there are always a few columns of unfilled pixels at the edges of the image.

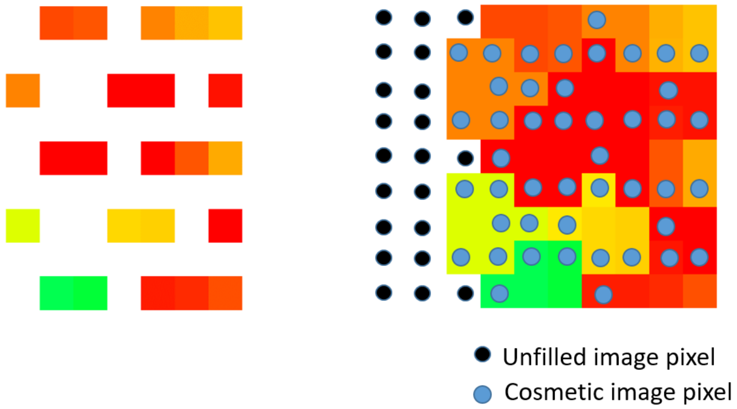

8.2.15 What is the difference between the different cloud masks in the Level-1 product?

There are several different cloud masks available in the Level-1 product:

Basic Level-1 cloud mask: The basic mask is a generic cloud mask based on a number of separate threshold and empirical based cloud tests. The results of 14 individual cloud tests (see the *L1 ATBD*) are provided in the 'cloud' variable within the 'flags' NetCDF file, and their combined result is provided in the 'summary_cloud' bit of the 'confidence' variable within the flags file. These tests identify clouds based on different physical properties and under different conditions. Therefore, not all cloud tests operate over all pixels, and there is a day/night, land/sea split. Some tests also depend on the results of previous cloud tests in the implementation chain. The number of cloud tests that identify cloud does not necessarily relate to a measure of confidence that there is cloud present. It can be helpful to investigate using only specific cloud tests according to user need, as for example, some clouds tests may be more prone to identifying aerosols.

Bayes cloud: In products generated prior to 20/02/22, the Bayes cloud variable contains the Level-2 Marine Bayesian cloud mask over ocean, and the Level-2 Land probabilistic cloud mask over land (see Section 6.2.1). These cloud masks are the same as provided in the Level-2 SST and LST products. In later processing baselines, after and including PB SL__L1_.004.04, this container is empty as the Bayes cloud is no longer included in the Level-1 product.

Note that the FRP cloud mask is not provided in the Level-1 product.

8.2.16 What does it mean if the pointing flag is raised?

Within the confidence word of the 'flags' NetCDF file there is a pointing flag. This is raised is any of the bits are set. Very infrequently, the flag relating to the scan mirror or flip mirror may be raised to indicated issues such as jitter. But in more cases, the 'platform mode' flag is raised. Circumstances under which this is activated include:

- Planned satellite manouvres such as when viewing the Moon for calibration purposes (once per 2 months for each of S3A, S3B)
- Collision avoidance manouvres, occur at random intervals

- Scheduled in-plane manoeuvre or out of plane manoeuvre

Details of these are provided in the monthly data quality reports. When the platform mode flag is raised it means the geolocation accuracy cannot be guarented to be the same as in a normal mode. The impact on the products can be minimal or can be significant, as shown in Figure 24

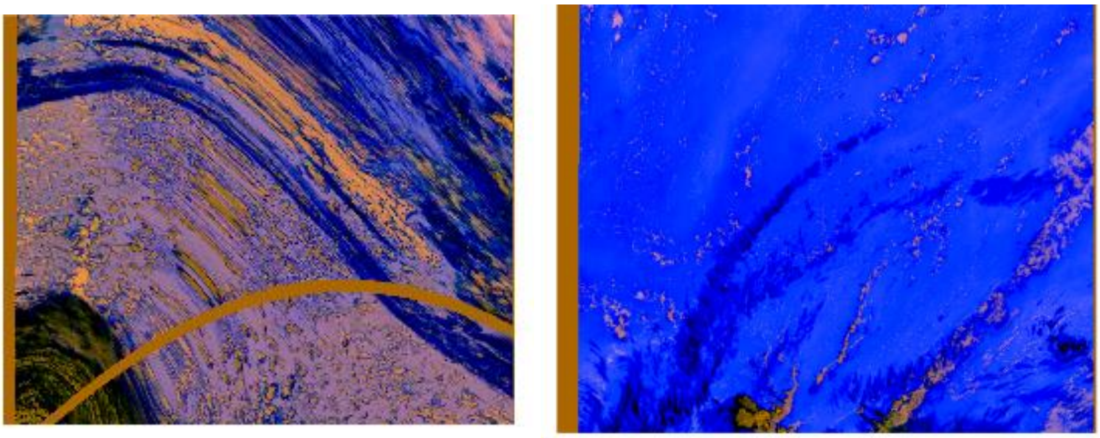

Figure 24. Left: S3B night-time image from 6th April 2022 during a Lunar manouvre, with the pointing model flag raised. Right: S3B image from 24th May 2022 during a scheduled manouvre, with the pointing mode flag raised. Thereis a clear degradation in image quality in the first case, but not in the second.

8.2.17 How do I find quality information in the product manifest?

There are two main quality indicators in the manifiest file.

- OnlineQualityCheck

It should be noted that this check is always marked as PASSED, regardless of the data quality. This is something that will be addressed in future evolutions of the product in order to make a more meaningful and useful flag.

- DegradationFlags

There are several different degradiation flags that are set during the processing of the Level-1 product. If any of these flags are set, they will appear in the manifest file as a list. For example, in this particular file we see that the INPUT_GAPS flag has been raised:

```
<sentinel3:degradationFlags>INPUT_GAPS</sentinel3:degradationFlags>
```

A description of the individual flags that might appear in the manifest is given below.

- INPUT_GAPS – raised if the NAVATT have gaps that can be filled by interpolation, and in this case, NAVATT files are listed as resources in the manifest
- ADF_GAPS – raised if there was a gap in ECMWF file coverage either side of the product *mid-point*
- NON_NOMINAL_ORBIT_INFO – NAVATT was not available or not usable and nonnominal orbit information was used instead
- MISSING_NAVATT - raised if no NAVATT packets were provided
- MANOEUVRES- Satellite manoeuvres took place during the measurement period of the product. Check the pointing flag in the confidence word.
- THRUSTS- satellite thrusts took place during the measurement period of the product.
- DISCARDED_NAVATT – raised if the provided NAVATT packets were discarded. In this *case the NAVATT files are not listed as resources in the manifest*

Note that these flags are not passed to the Level-2 products.

8.2.18 How do I calculate the per pixel uncertainty at Level 1?

Level-1 products contain uncertainty information in the quality datasets S<n>_quality_<vv>.nc

- Random effects - detector noise expressed as NEDT (TIR channels) and NEDL (VIS/SWIR channels) are provided for each scan line
- Correlated effects - radiometric calibration are included in the quality annotation datasets as a table of uncertainty vs. temperature type-B (a-priori) estimates based on the pre-launch calibration and calibration model

Per pixel uncertainty estimates can be derived by interpolating the values provided in the quality dataset to the BT/radiance values in each pixel for each channel.

To ease this process, a python tool has been developed to calcualate per pixel uncertainties. Further information and links to the code and documentation are available via https://www.eumetsat.int/S3-TIR-uncertainties.

8.3 If you have a question

The Services Coordinated Interface (SCI) is the user service dedicated to Copernicus users. The SCI handles the Copernicus users' enquiries, orders and complaints, and coordinates the data provision according to user requirements and data offer.

While Sentinel dedicated information is available in the present pages, the Copernicus Space Component Data Access system (CSCDA) web site is the entry point for obtaining information regarding the global data offer, available tools and data provisions status.

The SCI is available for user support; they can be contacted via email at EOSupport@copernicus.esa.int for support, in particular for:

- Clarifications regarding the registration process
- Sentinel enquiries
- Reporting issues related to products/service quality

8.4 Useful links

8.4.1 About Copernicus

- CSCDA: https://spacedata.copernicus.eu/
- EU Copernicus: https://www.copernicus.eu/en
- ESA Copernicus: http://www.esa.int/Applications/Observing_the_Earth/Copernicus

8.4.2 About ESA and the Sentinel missions

- ESA website: http://www.esa.int
- Sentinel Online: https://sentinel.esa.int/web/sentinel/home

8.4.3 About SLSTR

- User guides: https://sentinel.esa.int/web/sentinel/user-guides/sentinel-3-slstr
- Technical guide: https://sentinel.esa.int/web/sentinel/technical-guides/sentinel-3-slstr
- Processing Baseline information: https://sentinel.esa.int/web/sentinel/technical-guides/sentinel-3-slstr/processing-baseline
- Anomalies and Events related to SLSTR: https://sentinel.esa.int/web/sentinel/technical-guides/sentinel-3-slstr/anomalies-and-events
- Monthly data quality report: https://sentinel.esa.int/web/sentinel/technical-guides/sentinel-3-slstr/data-quality-reports

8.4.4 About S3 toolbox

- STEP: http://step.esa.int/main/download/
- Forum: https://forum.step.esa.int/

8.5 References

SLSTR documents available on the Sentinel Online website:

(https://sentinel.esa.int/web/sentinel/user-guides/sentinel-3-slstr/document-library)

- *L1 PDFS*: Sentinel-3 SLSTR Product Data Format Specification - Level 1 products
- *L2 PDFS*: Sentinel-3 SLSTR Product Data Format Specification - Level-2 Land products
- *L1 ATBD*: Sentinel-3 SLSTR Level-1 Observables ATBD
- *LST ATBD*: Sentinel-3 SLSTR Land Surface Temperature ATBD
- *FRP ATBD*: Sentinel-3 SLSTR - Active Fire: Fire Detection and Fire Radiative Power ATBD

- Arino, O., Gross, D., Ranera, F., *et al.* (2007), *GlobCover: ESA service for Global land cover from MERIS*, New York: Ieee
- Baret, F., Weiss, M., Lacaze, R., *et al.* (2013), GEOV1: LAI and FAPAR essential climate variables and FCOVER global time series capitalizing over existing products. Part1: Principles of development and production, *Remote Sensing of Environment, 137*, 299-309
- Coppo, P., Ricciarelli, B., Brandani, F., *et al.* (2010), SLSTR: a high accuracy dual scan temperature radiometer for sea and land surface monitoring from space, *Journal of Modern Optics*, 57, 1815–1830.
- Dee, D. P., Uppala, S. M., Simmons, A. J., *et al.* (2011), The ERA-Interim reanalysis: configuration and performance of the data assimilation system, *Quarterly Journal of the Royal Meteorological Society, 137*, 553-597
- Eastwood, S. & Andersen, S. 2007. Masking of Sea Ice for METOP SST retrieval. OSI SAF report.
- Freeborn, P. H., Wooster, M. J., Roberts, G., & Xu, W. D. (2014), Evaluating the SEVIRI Fire Thermal Anomaly Detection Algorithm across the Central African Republic Using the MODIS Active Fire Product, *Remote Sensing, 6*, 1890-1917.
- Ghent, D., Corlett, G., Goettsche, F., & Remedios, J. (2017), Global land surface temperature from the Along-Track Scanning Radiometers, *Journal of Geophysical Research – Atmospheres*, 122, 12167-12193
- Hunt, S. E., Mittaz, J. P. D., Smith, D., *et al.* (2020), Comparison of the Sentinel-3A and B SLSTR Tandem Phase Data Using Metrological Principles, *Remote Sensing,* 12, 2893.
- Giglio, L. (2007), Characterization of the tropical diurnal fire cycle using VIRS and MODIS observations, *Remote Sensing of Environment, 108*, 407-421.
- Giglio, L., Descloitres, J., Justice, C. O., & Kaufman, Y. J. (2003), An Enhanced Contextual Fire Detection Algorithm for MODI, *Remote Sensing of Environment*, *87*, 273-282.
- Istomina, L. G., von Hoyningen-Huene, W., Kokhanovsky, A. A., and Burrows, J. P.: The detection of cloud-free snow-covered areas using AATSR measurements, Atmos. Meas. Tech., 3, 1005–1017, https://doi.org/10.5194/amt-3-1005-2010, 2010

- Nguyen, H. M., & Wooster, M. J. (2020), Advances in the estimation of high Spatio-temporal resolution pan-African top-down biomass burning emissions made using geostationary fire radiative power (FRP) and MAIAC aerosol optical depth (AOD) data, *Remote Sensing of Environment*, 248, 111971.
- Roberts, G., Wooster, M. J., & Lagoudakis, E. (2009), Annual and diurnal african biomass burning temporal dynamics, *Biogeosciences*, *6*(5), 849-866.
- Sessa, R. (Ed.). (2008), *Terrestrial Essential Climate Variables: For Climate Change Assessment, Mitigation and Adaptation*, GTOS-Secr., Food and Agriculture Organization of the United Nations.
- Smith D. (2020), Assessment of Visible and Short Wavelength Radiometric Calibration using Vicarious Calibration Methods, Sentinel-3 MPC Techncial Document, S3MPC.RAL.TN.010.
- Smith, D., Barillot, M., Bianchi, S., *et al.* (2020), Sentinel-3A/B SLSTR Pre-Launch Calibration of the Thermal InfraRed Channels., *Remote Sensing*, 12, 2510.
- Thuillier, G., Hersé, M., Labs, D., *et al.* (2003), The Solar Spectral Irradiance from 200 to 2400 nm as Measured by the SOLSPEC Spectrometer from the Atlas and Eureca Missions, *Solar Physics*, 214, 1-22.
- Wooster, M.J., Zhukov, B., & Oertel, D. (2003), Fire radiative energy for quantitative study of biomass burning: derivation from the BIRD experimental satellite and comparison to MODIS fire products, *Remote Sensing of Environment*, 86, 83-107.
- Wooster, M. J., Roberts, G., Perry, G. L. W., & Kaufman, Y. J. (2005), Retrieval of biomass combustion rates and totals from fire radiative power observations: FRP derivation and calibration relationships between biomass consumption and fire radiative energy release, *Journal of Geophysical Research: Atmospheres*, 110(D24).
- Wooster, M. J., Xu, W., & Nightingale, T. (2012), Sentinel-3 SLSTR active fire detection and FRP product: Pre-launch algorithm development and performance evaluation using MODIS and ASTER datasets, *Remote Sensing of Environment*, 120(0), 236-254.
- Wooster, M.J., Roberts, G., Freeborn, P.H., *et al.* (2015), LSA SAF Meteosat FRP products–Part 1: Algorithms, product, *Atmos. Chem. Phys*, *15*(22), 13217-13239.
- Xu, W., Wooster, M. J., He, J., & Zhang, T. (2020), First study of Sentinel-3 SLSTR active fire detection and FRP retrieval: Night-time algorithm enhancements and global intercomparison to MODIS and VIIRS AF products, *Remote Sensing of Environment*, 248, 111947.

8.6 Acronyms and abbreviations

ADF ---------------Auxiliary Data File

AF -----------------Active Fire

ANX---------------Ascending Node Crossing

API ----------------Application Programming Interface

ATBD -------------Algorithm Theoretical Basis Document

(A)ATSR ----------(Advanced) Along Track Scanning Radiometer

BB-----------------Blackbody

BT -----------------Brightness Temperature

BTD ---------------Brightness Temperature Difference

CSCDA------------Copernicus Space Component Data Access

CNES -------------Centre National d'études Spatiales

DIAS --------------Copernicus Data and Information Access Service

ECMWF----------European Centre for Medium-Range Weather Forecasts

ECV ---------------Essential Climate Variable

ESA ---------------European Space Agency

FRP ---------------Fire Radiative Power

IPF ----------------Instrument Processing Facility

LSA SAF ----------Satellite Application Facility on Land Surface Analysis

LSE----------------Land Surface Emissivity

LST----------------Land Surface Temperature

MIR---------------Middle Infrared

MERIS------------MEdium Resolution Imaging Spectrometer

MODIS -----------Moderate Resolution Imaging Spectroradiometer

NaN---------------Not a Number

NASA -------------National Aeronautics and Space Administration

NDVI--------------Normalized Difference Vegetation Index

NEDT -------------Noise Equivalent Delta Temperature

NEDL -------------Noise Equivalent Delta Radiance

NetCDF ----------Network Common Data Format

NRT---------------Near Real Time

NTC---------------Non Time Critical

OLS ---------------Ordinary Least Squares

PDFS--------------Product Data Format Specification

PDU---------------Product Dissemination Unit pdf ----------------probability density function

POD --------------Precise Orbit Determination

PRT ---------------Platinum Resistance Thermometer

RAL ---------------Rutherford Appleton Laboratory

RBT ---------------Radiance Brightness Temperature

SAFE --------------Standard Archive Format for Europe

SCI ----------------Services Coordinated Interface

SLSTR-------------Sea and Land Surface Temperature Radiometer

SNAP -------------Sentinel Applications Platform

SST----------------Sea Surface Temperature

STEP --------------Science Toolbox Exploitation Platform

SWIR -------------Shortwave Infrared

TCWV ------------Total Column Water Vapour

TIR ----------------Thermal Infrared

ToA ---------------Top of Atmosphere

VIS ----------------Visible

VISCAL ----------Visible Calibration source

UTC ---------------Coordinated Universal Time

XML---------------Extensible Markup Language